Core Complex Segmentation in North Aegean, A Dynamic View

Dimitrios Sokoutis, Jean-Pierre Brun

Tectonics

RESEARCH ARTICLE
10.1029/2017TC004939

Special Section:
Geodynamics, Crustal and Lithospheric Tectonics, and active deformation in the Mediterranean Regions (A tribute to Prof. Renato Funiciello)

Core Complex Segmentation in North Aegean, A Dynamic View

Jean-Pierre Brun[1] and **Dimitrios Sokoutis**[2,3]

[1]Univ Rennes, CNRS, Géosciences Rennes—UMR 6118, Rennes, France, [2]Faculty of Earth Science, Utrecht University, Utrecht, Netherlands, [3]Department of Geosciences, University of Oslo, Oslo, Norway

Abstract The core complexes of the North Aegean result from the gravity spreading of a thrust wedge, driven by the Hellenic slab rollback, since middle Eocene. The development of the Southern Rhodope Core Complex occurred in two stages: (i) core complex exhumation accommodated by the Kerdylion detachment and (ii) steep normal faulting controlling the deposition of Neogene sedimentary basins that segmented the core complex. Both stages have been controlled by a clockwise rotation of the detachment hanging wall. The bulk amount of extension along the Aegean coastline in Northern Greece reached 120 km. The transition between the two stages occurred in middle Miocene due to an increase in extensional displacement by a factor 5. This transition between two different modes of extension, from localized detachment (i.e., core complex mode) to distributed steep normal faulting (i.e., wide rift mode), occurred at Aegean scale as a result of an acceleration of slab rollback. The Neogene basins emplaced close to the detachment, where brittle upper crust was thin (around 7 km) but containing weak marble layers allowing the formation of ramp-flat extensional systems with rollover-type basin fill. Since Pliocene, the stretching direction changed, from NE-SW to NS, due to the propagation of the North Anatolian Fault in the North Aegean domain.

Key Points:
- Core complexes of the North Aegean resulted from large-scale extension driven by slab rollback
- The Southern Rhodope Core Complex exhumed below the Kerdylion detachment since middle Eocene and was segmented by wide rifting since middle Miocene
- Wide rift extension resulted from an increase in stretching rate by a factor 5, powered by an acceleration of trench retreat

Correspondence to:
J.-P. Brun,
jean-pierre.brun@univ-rennes1.fr

Citation:
Brun, J.-P., & Sokoutis, D. (2018). Core complex segmentation in North Aegean, a dynamic view. *Tectonics*, *37*. https://doi.org/10.1029/2017TC004939

Received 20 DEC 2017
Accepted 1 MAY 2018
Accepted article online 9 MAY 2018

1. Introduction

The Southern Rhodope Core Complex (SRCC) in the North Aegean with a width up to 120 km parallel to the stretching direction (Figure 1a) belongs to the largest core complexes identified worldwide. It initiated in middle Eocene and amplified during around 30 Myr and was suddenly interrupted in middle Miocene by a wide rift event that segmented it in several units (Brun & Sokoutis, 2007). The cause of this major change in extension mode that remained not understood since long is well illustrated by the history of back-arc extension in the Aegean (Brun et al., 2016; Figure 1b). The present paper aims at documenting that the structural and kinematic study of Neogene basins, which were deposited on top of rocks exhumed in the core complex during this segmentation event, and their relation with other basins of the same age at Aegean scale support that an increase of extension rate occurred in middle Miocene.

Back-arc extension in the Aegean, driven by slab rollback (Brun & Faccenna, 2008; Brun & Sokoutis, 2010; Faccenna et al., 2003, 2014; Jolivet & Brun, 2010; Jolivet & Faccenna, 2000; Royden, 1993), occurred into two main stages with very different large-scale deformation mechanisms and velocities of displacement estimated by restoration (Brun et al., 2016). During the first stage, from middle Eocene to middle Miocene (Figure 1b), the velocity of trench retreat was around 0.6 cm/yr. Slow rate of stretching was accommodated by localized deformation leading to the exhumation of (i) high-pressure metamorphic rocks (i.e., Cycladic Blueschists) and (ii) metamorphic core complexes (i.e., SRCC and Central Cycladic Core Complex; Figure 1a). Associated sedimentary basins are located in the northern and central parts of the Aegean domain (Thrace Basin: Görür & Okay, 1996; Thermaïkos Basin: Roussos, 1994; Mesohellenic Trough: Ferrière et al., 2004). During the second stage, since middle Miocene, the velocity of trench retreat progressively accelerated to reach 3.2 cm/yr during the last 5 Ma (Brun et al., 2016), very close to the present-day velocities measured in Crete (McClusky et al., 2000). Crustal extension that was localized, during exhumation of high-pressure metamorphic rocks and core complexes, became distributed, leading to the deposition of Neogene basins at the scale of the whole Aegean domain, both onshore (Bornovas & Rondogianni-Tsiambaou, 1983) and offshore (Mascle & Martin, 1990).

An important geological consequence of this strong change in the mechanism of Aegean back-arc extension that occurred in middle Miocene is the segmentation of the large domains of metamorphic rocks, exhumed

10.1029/2017TC004939

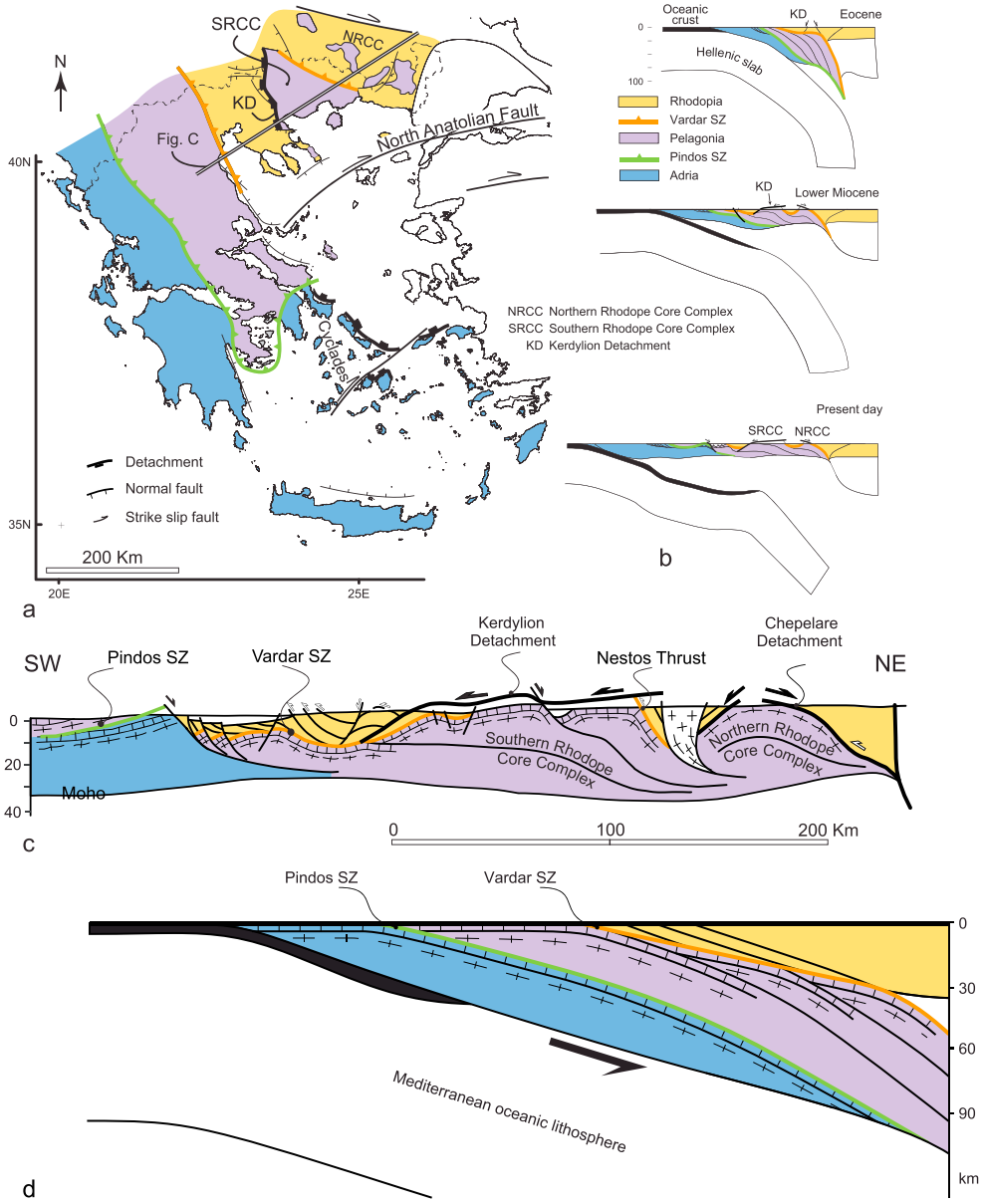

Figure 1. (a) General setting of the Northern (NRCC) and Southern (SRCC) Rhodope Core complexes in the frame of the Aegean back-arc extensional system. (b) Lithosphere scale cross sections showing the two main stages of Aegean extension, from Eocene to lower Miocene and from middle Miocene to present day (a and b modified after Brun et al., 2016). (c) Regional cross section of the North Aegean domain showing the structural setting at crustal-scale of the NRCC and SRCC. (d) Approximate restoration of section c showing the thrust wedge geometry in middle Eocene, prior to the onset of core complex extension.

during the first stage, by combined systems of normal and strike-slip faults that controlled the deposition of Neogene basins (Brun et al., 2016). Therefore, the lateral continuity of the metamorphic units, either of high pressure (i.e., blueschist and eclogites) or high temperature (i.e., gneisses and migmatites) became obscured by superposed younger extensional structures and largely hidden by associated Neogene sediments when they have not subsided under the sea level, leaving only restricted parts of them accessible in islands, like in the Cyclades (Philippon et al., 2012). The two deformation stages were both extensional with their principal strain directions often trending close to each other what renders their separation in the field often difficult and sometimes impossible. The geological complexities that result from the superposition of these two stages of extension are likely responsible for some misconceptions concerning the deformation

processes involved in Aegean extension as well as their organization in time (since 45 Ma) and in space (over the whole Aegean domain). This is well illustrated in core complex areas, as the fault patterns that controlled the deposition of Neogene basins are seen to result from stretching directions trending parallel or at small angle to stretching lineations in the neighboring metamorphic rocks. As a consequence, it has often been concluded (i) that the core complex development was coeval with the formation of Neogene basins and (ii) that the contact between Neogene sediments and the underlying metamorphic rocks were detachments controlling core complex exhumation. This is exemplified in the SRCC that initiated in mid-Eocene (Brun & Sokoutis, 2004, 2007). However, when this core complex was initially identified (Dinter & Royden, 1993; Sokoutis et al., 1993), its development has been considered to occur dominantly during the Neogene and the contact between the Neogene sediments and the underlying metamorphic rocks has been interpreted as a major detachment, so-called "Strymon Valley Detachment" (Dinter & Royden, 1993), responsible for the exhumation of the core complex. This type of misinterpretation had and still has obvious consequences in terms of regional geology, in particular concerning the history and kinematics of Aegean extension at large scale. In terms of processes, it also overlooks the mechanical significance of the rather sudden transition from core complex to wide rift (with multiple extensional basins) modes of extension—that is, from a localized to a distributed mode of extension—that characterizes the Aegean back-arc extension (Brun et al., 2016). At variance with the Cyclades that dominantly outcrop undersea, the SRCC largely outcrops inland allowing easy observation of faulting and related sedimentary basins associated to the core complex segmentation.

The present paper, after a review of the SRCC, focuses on the deformation mechanisms involved in the segmentation of the SRCC by the superposed event of wide rifting during Neogene. Our field study of the SRCC is documented by (i) maps of the deformation zones that segment the core complex and of the associated Neogene basins, (ii) deformation patterns and structures that characterize these deformation zones, and (iii) geochronological data that provide constraints on their timing of development together with stratigraphy of basin infilling. It is shown that the development of several Neogene basins in the region was controlled by ramp-flat extensional systems. These results are used to discuss the kinematics and mechanical processes of Neogene extension in the North Aegean and the rheological implications at crustal scale. It is argued that an increase in stretching rate by a factor 5 has been responsible for a transition from core complex to wide rift modes of extension, leading to a segmentation of the SRCC and controlling the deposition of Neogene sedimentary basins.

2. Core Complex Extension in the Rhodope

2.1. General Setting

The core complexes of the Rhodope consist in two main structures (Figures 1a and 1c): (i) an alignment of four small domes in Northern Rhodope (namely, Chepinska, Arda, Kesebir-Kardamos, and Biela-Reka-Kechros; see review in Burg, 2011) that, for convenience, are called here "Northern Rhodope Core Complex" (NRCC) and (ii) a larger triangular shape structure in Southern Rhodope called SRCC (Brun & Sokoutis, 2007) (Figures 1a and 1c). Extension, which started in Eocene, as recently reviewed by Burchfiel et al. (2008) and Burg (2011), affected a large thrust wedge resulting from the subduction of the Pelagonia and Adria continental blocks below Rhodopia (Brun et al., 2016; Figure 1b) that previously recorded one (or several) tectonic and metamorphic cycle(s) in Mesozoic (Burg, 2011; Burg et al., 1996; Ricou et al., 1998). The NRCC and SRCC likely initiated almost simultaneously in middle Eocene. But whereas the exhumation of the NRCC decayed and stopped in lower Oligocene, as indicated by the end of southwest-directed shear in the Nestos Thrust area (Nagel et al., 2011) and the similar low temperature dating on both sides of it (Kounov et al., 2015), the SRCC continued to develop up to early Miocene, cutting Rhodopia in two domains (Figure 2): (i) North Rhodopia and (ii) Southwest Rhodopia (Chalkidiki peninsula). Progressive exhumation of the SRCC occurred in dextral rotation (Brun & Sokoutis, 2007), as implied by differential rotation of North and Southwest Rhodopia documented by paleomagnetic data (Dimitriadis et al., 1998; Kissel & Laj, 1988), giving its characteristic triangular shape to the core complex in map view (Figure 2), with an extensional displacement reaching 120 km along the Aegean coastline in a mean NE-SW direction.

North Rhodopia, located to the north of the Nestos Thrust (Figure 2), recorded a long and complicated tectonic history resulting from the superposition of one or several events of thrusting and extensional exhumation of ultrahigh pressure metamorphic rocks during Mesozoic and Aegean extension during early Tertiary,

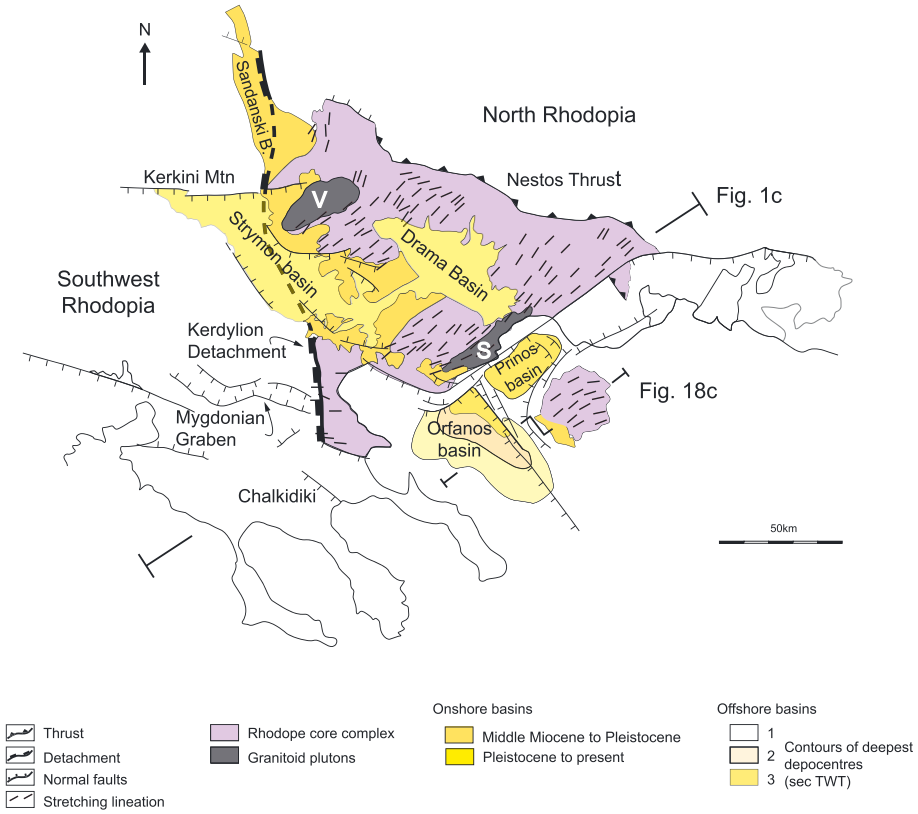

Figure 2. Simplified geological map of the Southern Rhodope Core Complex and the Neogene sedimentary basins. V: Vrondou pluton. S: Symvolon pluton.

leading to the development of the NRCC (Figure 1), with associated sedimentation and volcanism (Burg, 2011; Fytikas et al., 1984). In strong contrast with this, the metamorphic units of the Southwest Rhodopia (Chalkidiki peninsula; Figure 2) that are comparable to those of North Rhodope (Kydonakis, Brun, Sokoutis, & Gueydan, 2015) were exhumed in Eocene (Kydonakis et al., 2014) and, since then, have been only slightly affected by Tertiary extension, mainly by the Mygdonian graben (Figure 2) whose development started in middle Miocene (Kydonakis, Brun, Sokoutis, & Gueydan, 2015).

2.2. Remark

Since the identification of the SRCC in 1993, made simultaneously by Dinter and Royden and by Sokoutis and coworkers, nearly all following works carried out in the Greek and Bulgarian Rhodope brought a wealth of data (geological and structural mapping, petrology, kinematic analysis of ductile deformation, and high and low temperature geochronology; see review in Burg, 2011) that confirmed the core complex interpretation and improved the understanding of the structure and development of the SRCC and the NRCC. However, it must be quoted that some recent works put in question the existence of the core complexes (i.e., the extensional exhumation of high temperature metamorphic rocks) and the associated detachments in the Rhodope. However, these criticisms were made on the only basis of brittle deformation (i.e., fault slip analysis; e.g., Tranos, 2011, 2016) or combining geomorphology, low temperature dating, and faulting (so-called "landscape analysis"; e.g., Gunnell et al., 2017). Surprisingly, those two types of approaches that challenge the evidence for core complex-type extension in the Rhodope fully discard all types of data sets that are of primary importance for the identification of core complexes: metamorphism, ductile deformation, and high temperature geochronology. Simultaneously, objections raised against the "MCC theory" (term used by Gunnell et al., 2017) are based on observations and data that solely concern the postmetamorphic evolution of the Rhodope (i.e., brittle deformation (Gunnell et al., 2017; Tranos, 2011, 2016; Tranos et al., 2009) and erosion landscapes (Gunnell et al., 2017), whereas the development of a core complex is necessarily syn-metamorphic.

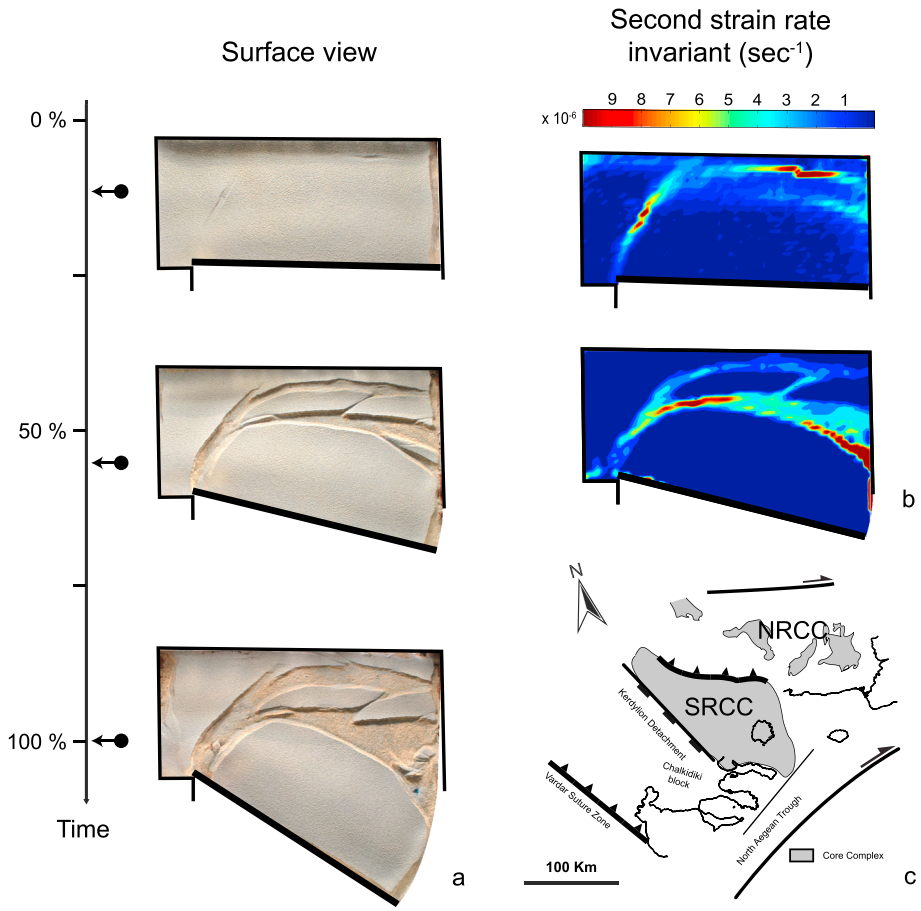

Figure 3. Analogue modeling of core complex development in the North Aegean as resulting from the gravity spreading of a thrust wedge (modified after Kydonakis, Brun, & Sokoutis, 2015). (a) Three surface views of a model showing the progressive development of two core complex domains during the displacement in dextral rotation of the mobile boundary (thick black line). (b) Maps of the second strain rate invariant calculated at the onset of extension (up) and close to half of the bulk extension (down) showing the location of maximum strain rate intensity (in red). (c) Simplified map of the two domains of core complexes in the Rhodope (Northern Rhodope Core complex and Southern Rhodope Core Complex). Compare with the model top view at the end of experiment (a down; 100%).

2.3. Dynamics of Core Complex Development

Restoration of Aegean extension at lithosphere scale (Brun et al., 2016; Figure 1b). shows the structure of the thrust wedge prior to extension in Eocene that resulted from the successive subduction of Pelagonia and Adria below Rhodopia. As a consequence of the Hellenic slab rollback starting in Paleocene-Eocene, crust-mantle delamination put the crustal wedge base in direct contact with the asthenosphere (Brun & Faccenna, 2008; Tirel et al., 2013). Consequently, the lower units of the thrust wedge were rather suddenly strongly heated and underwent partial melting. This is likely responsible for the intrusion, in the Nestos thrust hanging wall, of early to middle Tertiary granitic plutons, mostly calc-alkaline (Jones et al., 1992) and mixing deep crust and mantle sources (von Quadt & Peytcheva, 2005). However, instead of mantle delamination during slab rollback, a more classical process of mantle upwelling is invoked to explain the nature and geochemical signature of these plutons (Pe-Piper & Piper, 2006; Schenker et al., 2012). Two core complex domains (NRCC and SRCC) initiated in Eocene, but the NRCC exhumation decayed and stopped in early Oligocene, whereas the SRCC exhumation continued up to early Miocene.

Analogue modeling of thrust wedge extension with initial and boundary conditions adapted to the Rhodope example provides a simple first-order mechanical explanation to the development of core complexes in the Rhodope (Kydonakis, Brun, & Sokoutis, 2015).

Wedge-shaped models were built with sand and silicone polymer to represent the upper brittle crust and the middle-lower crust, respectively respecting the classical scaling procedure for this type of models (e.g., Brun, 1999). A mean 20° initial wedge angle was chosen on the basis of our restored crustal-scale cross sections of the North Aegean (Figure 1b). Extensional displacement was applied at constant rate to the thinner wedge end by a rotating wall, to take into account the differential block rotation demonstrated by paleomagnetism in the Rhodope (see section 2.1). The wedge model lying on top of a rigid plate initially inclined of 20° was progressively rotated toward horizontal to simulate an isostatic readjustment as a function of extension and thinning. At the onset of experiment the wedge surface was inclined of 3° toward the mobile wall to simulate the topography, higher above the thickest part of the wedge (corresponding to 70 km in nature).

Three top views of a model (Figure 3a) illustrate the progressive development of extensional structures with strain rate maps for the two first stages (Figure 3b). The model shows (i) that two core complexes develop in the thicker part of the wedge, (ii) that the northern one (north being the figure upper part) opens less than the southern one, (iii) that the southern one opens in rotation, and (iv) that a large block remained nondeformed against the rotating wall, above the thinner part of the wedge. The second-stage strain rate map shows that higher strain rates are located against the southern rotating block, corresponding to the zone of most active deformation (i.e., the detachment zone). The final top view fairly compares to the Rhodope (Figure 3c) with its two core complex domains (NRCC and SRCC), the largest domain of exhumed ductile crust in the SRCC, the location of the Kerdylion detachment to its southern side, and the southern block remaining nondeformed until late Miocene.

Contrary to comparable previous analogue models carried out with the same technique but not initially wedge-shaped (Brun et al., 1994; Tirel et al., 2006) there is no anomaly of viscosity introduced in the ductile layer to stimulate core complex location. The initiation of extension occurs at wedge rear, away from the moving boundary, because the thickest wedge part is where buoyancy forces and related isostasy are the highest. In addition, even if likely of lesser importance, it is also where ductile strength (i.e., strain rate × viscosity) is the lowest as, for a given displacement velocity, strain rate decreases with increasing thickness (see strength profiles; Figure 6 in Kydonakis, Brun, & Sokoutis, 2015).

In this laboratory model, extension results from the gravity spreading of a BD wedge controlled by displacement at constant rate of its frontal boundary. This supports that Aegean extension corresponds to the gravity collapse, driven by slab rollback, of a thrust wedge that resulted from the pilling up of continental crust units in the subduction zone that closed the Vardar and Pindos oceans.

3. The Southern Rhodope Core Complex

The SRCC domain concerned by the present study (Figure 4) is characterized by high reliefs, made of metamorphic and plutonic rocks exhumed from middle Eocene to lower Miocene, whose present-day altitude reaches 2,000 m (e.g., Pangeon and Falakron mountains) and by sedimentary basins deposited since middle Miocene among which some are inverted and deeply eroded (e.g., Serres) reaching moderate altitudes, lower than 1,000 m, while others are still subsiding with flat surfaces close to sea level (e.g., Strymon and Drama basins) (Figure 4a).

The SRCC is bound to the north by the Nestos Thrust and to the south by the Kerdylion detachment (Brun & Sokoutis, 2007). The Tertiary extensional history of the SRCC occurred in two main steps: (i) exhumation of the core complex (s.s.) from middle Eocene and (ii) segmentation of the core complex during the Neogene. This section summarizes the evolution of the core complex from middle Eocene to early Miocene.

3.1. Core Units

The core of the SRCC is made of two types of geological units (Figure 4b): (i) a lower and dominant unit most often called "Pangeon-type" and (ii) an upper and smaller unit, located to the southwest of the SRCC here called "Kerdylion type."

"Pangeon-type unit" appelation is, for convenience, also used for identical units in the Menikion, Falakron, and Lekani mountains that surround the Drama basin and for the Thassos island. The Pangeon-type unit is made of (i) a thick cover pile of marbles, micaschists, and amphibolites whose base is possibly late Paleozoic (corresponding to the "Pangeon carbonate platform" of Papanikolaou, 2013; see his Figure 6), lying on top of (ii) orthogneisses, whose protolith corresponds to late Hercynian granites (with ages ranging

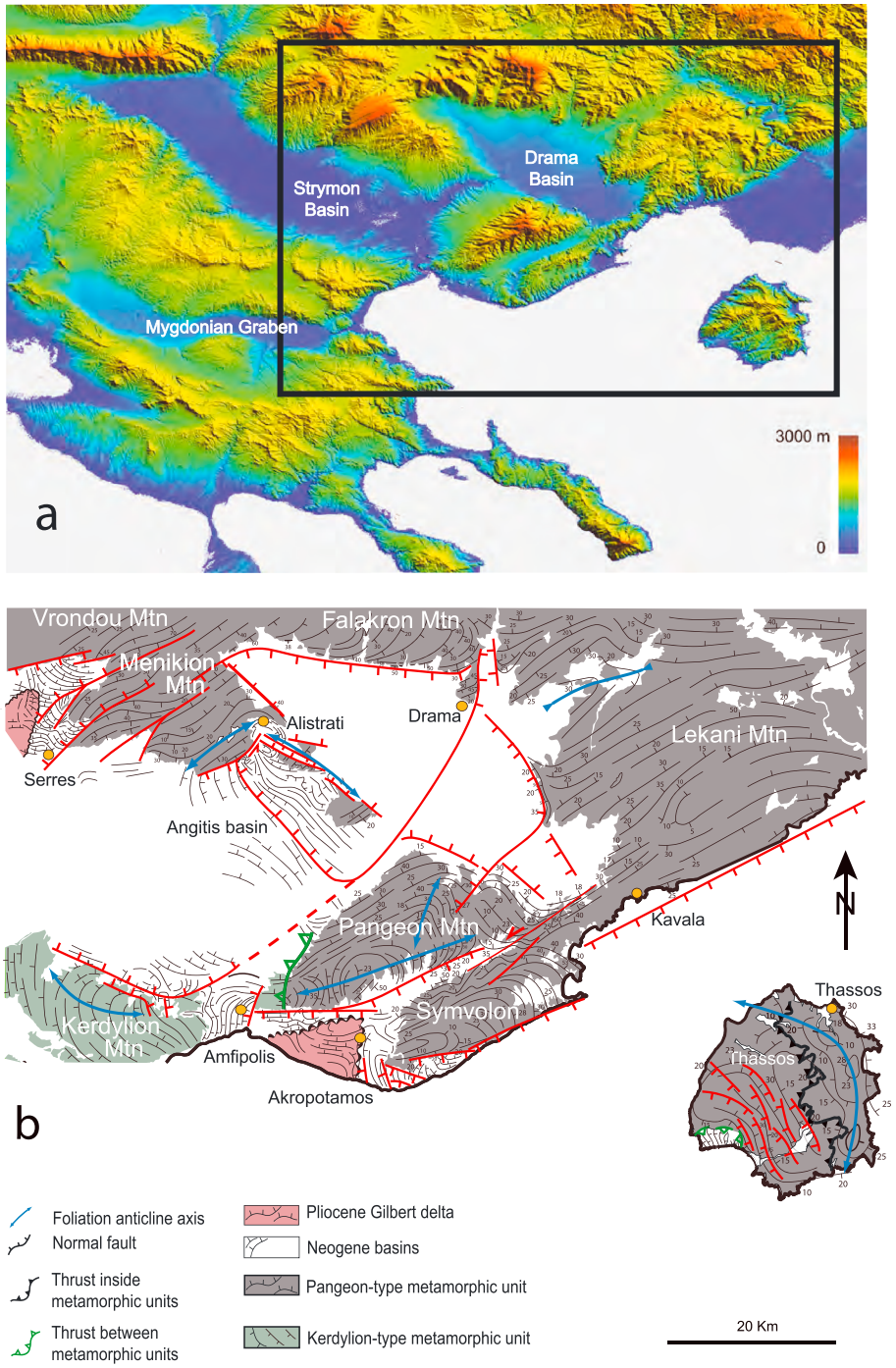

Figure 4. Topography, (a) internal structure of the Southern Rhodope Core Complex (foliation trajectories) and (b) normal faults related to the Neogene basins. Structural map b shown by a rectangle in topographic map a.

between 270 and 310 Ma throughout the Greek Rhodope: Wawrzenitz & Krohe, 1998; Liati & Gebauer, 1999; Turpaud & Reischmann, 2010; Liati, 2005) and paragneisses derived from Paleozoic sediments. The stratigraphic age of the whole meta-sedimentary pile is unknown, but they most likely represent peri-Tethys sedimentary and volcanic formations deposited on top of the Hercynian basement.

In the Pangeon-type unit, the Hercynian basement is often observed lying on top of marble layers in Falakron and Lekani mountains. Duplications of this type result from thrusting that affected both basement and cover.

This is especially well exemplified in the Thassos island where a large (20 × 15 km) and thin (maximum 3–4 km) SW-dipping slab, made of Hercynian basement gneisses covered by marbles, is lying on top of a thick pile of meta-sediments dominantly made of marbles (see geological map of Thassos; Figure 5 in Brun & Sokoutis, 2007). This abnormal superposition of older on younger demonstrates the thrust nature of the basal contact of gneisses with the underlying marbles.

"Kerdylion-type unit" appellation introduced here for the first time is made of biotite gneisses and migmatites with numerous intercalations of amphibolites and marble layers. Like in the Pangeon-type unit these intercalations likely result from thrusting. The gneisses and migmatites represent three distinct pulses of magmatism in Permo-Carboniferous (309–280 Ma), late Jurassic (142–160 Ma), and early Tertiary (72–47 Ma; Himmerkus et al., 2006). Of particular interest is the component of late Jurassic magmatism that is made of I-type granitoids generated at an active continental margin—that is, magmatic arc—and that has never been found in the Pangeon-type unit. This magmatic arc component can likely be correlated with the Chortiatis magmatic suite that makes the southern border of Southwest Rhodopia (Chalkidiki peninsula; Figure 2; Kydonakis, Brun, Sokoutis, & Gueydan, 2015).

3.2. Kerdylion Detachment

The exhumation of both Pangeon-type and Kerdylion-type units has been controlled by the Kerdylion detachment that trends NNW-SSE to the western side of the SRCC (Brun & Sokoutis, 2007). The footwall rocks located immediately below the detachment correspond to a thick pile of mylonites and ultramylonites, with cataclasites at the top, dipping as a mean by 30° to the west southwest (WSW). The detachment separates the gneisses and migmatites of the Kerdylion massif from the gneisses of the Serbo-Macedonian of the Chalkidiki peninsula. The Kerdylion Detachment initiated the exhumation of the SRCC at the latest at 42 Ma (Kounov et al., 2015). The northward extend of the detachment is hidden below sediments in the Strymon basin where it is likely offset by normal faults. Toward the north it corresponds to the contact between the Serbo-Macedonian gneisses of the Kerkini mountain and the SRCC and then likely joins the major normal fault that controlled the deposition of the Sandansky sedimentary basin on its eastern side (Figure 2).

Brun and Sokoutis (2007) provided detailed field arguments, in particular from Thassos, showing that the so-called Strymon Detachment (Dinter & Royden, 1993) is primarily a thrust fault (Kockel & Walther, 1965; Kockel et al., 1977) that has only been moderately reactivated in extension during late Neogene (Weingartner & Heijl, 1994) and Messinian-Pliocene sediment deposition (Lyberis & Sauvage, 1985). Nevertheless, since 2007 the Strymon Detachment has been quoted in many works and, recently, argued on the basis of low-temperature dating (Kounov et al., 2015). Consequently, (i) we reiterate and expand in Appendix A the arguments that plead against the existence of the Strymon Detachment, and (ii) the tectonic significance of this fault zone called "Strymon Thrust" is discussed below (section 3.4).

3.3. Deformation of Core Complex Rocks and Kinematics of Exhumation

3.3.1. Deformation

All rocks of the Pangeon-type unit are all strongly deformed at high temperature. In Thassos, kyanite-sillimanite bearing micaschists and paragneisses at the top of basement unit yield PT conditions of 5.5 ± 1.5 Kb and 600 ± 50°C (Dimitriadis, 1989), more broadly of pressure higher than 7 Kb and temperature higher than 600°C (Wawrzenitz & Krohe, 1998), and show evidence of partial melting (Brun & Sokoutis, 2007). In addition, inclusions of rutile in garnet and by biotite and plagioclase symplectites which may have replaced earlier phengite in garnet-bearing metabasites suggest that pressure may have been higher than about 12 Kb (Wawrzenitz & Krohe, 1998). Therefore, at the onset of extension the top of basement gneisses was at a temperature higher than 600°C and at a depth at least of 25 km and possibly up to 45 km.

Basement gneisses are everywhere strongly deformed leading to a strong mylonitic banding that resulted from strong shearing of original compositional heterogeneities (e.g., various granitic compositions, aplite and pegmatite dykes, inclusions) and variable amounts of grain size reduction during mylonitization. Most rocks of the Pangeon-type unit, except strongly recrystallized dolomitic marbles, commonly display (i) a layer parallel foliation; (ii) well-defined stretching lineations; (iii) shear indicators (dominantly C′-type shear bands), and less frequently rolling porphyroclasts and pressure shadows around clasts; (iv) isoclinal folds with axes parallel or at small angle to the stretching lineation and rather frequent sheath folds (indicating high values of principal stretching axis λ_1, i.e., high-strain intensities with a value of λ_1 commonly higher than 4.0); and (v)

rather common boudinage. At core complex scale stretching lineations display a rather constant NE-SW trend (Figure 2). As thrusting and core complex extension have directions of stretching close to each other and the same sense of shear top-to-SW, planar and linear fabrics resulting from each one of these two successive deformation events are in general impossible to separate. In other terms, deformation fabrics of the SRCC must be considered as thrusting-extension composite fabrics except in the Oligocene-early Miocene granite plutons. The strong mylonitic deformation of the Symvolon granite, locally up to ultramylonites, indicates that Tertiary deformation was strong enough to have reoriented any previous linear fabric whose obliquity with the Tertiary direction of stretching would have been up to 30°.

3.3.2. Kinematics

Stretching lineations that trend dominantly in an NE-SW direction define an arcuate pattern within the triangular shape of the SRCC at map scale (Figure 2) that we relate to the rotational displacement of the detachment hanging wall during core complex exhumation (see Figures 17 and 18 in Brun & Sokoutis, 2007). Lineations are almost systematically associated to senses of shear top-to-SW, compatible with the timing of exhumation younger toward the southwest, from the Nestos Thrust to the Kerdylion Detachment.

3.3.3. Timing of Exhumation

At the northern end of the SRCC, the Mesta graben indicates that in northern Rhodope extension started in middle-late Eocene (Burchfiel et al., 2003). The exhumation of the core complexes of Kesebir and Byala Reka was accompanied by widespread cooling of footwall rocks in middle to late Eocene between (42–37 Ma; Bonev, 2006). To the west of the SRCC, the Kerdylion Detachment initiated at the latest at 42 Ma (Kounov et al., 2015).

From mid-Eocene to mid-Oligocene the marble and gneisses of Pangeon-type exhumed in Falakron and Lekani and gneisses and migmatites with numerous marble layers in the Kerdylion area. From late Oligocene to early Miocene, the granitic plutons of Vrondou and Symvolon were emplaced synkinematicaly in the central-southern part of the core complex. The Menikion and Pangeon areas, where the two plutons were emplacing, and Thassos Island were exhumed during this period. The Symvolon pluton (Dinter et al., 1995) (see location in Figure 2), the small Elaion stock (located to the southern border of the Menikion mountain; Figure 4b), and the Vrondou pluton (see location in Figure 2; Kolocotroni & Dixon, 1991) display C/S mylonitic fabrics, along pluton contact with the country rocks, that indicate, contrary to C′-type fabrics, that emplacement and mylonitization were synchronous (Berthé et al., 1979; Gapais, 1989). The emplacement depth of the Vrondou pluton has been estimated from the PT conditions at depths corresponding to 2–3 kb—that is, around 8–11 km (Kolocotroni & Dixon, 1991). An Oligocene-lower Miocene timing of emplacement is given by $^{39}Ar/^{40}Ar$ ages of 29.0 ± 0.7 Ma and 30.0 ± 0.4 Ma for Eastern Vrondou pluton (Figure 2) and Elaion stock (Kaufman, 1995) and a U-Pb Titanite age of 23.7 ± 0.1 and a $^{39}Ar/^{40}Ar$ cooling age of 22 ± 2 Ma for central Vrondou (Kaufman, 1995). U-Pb Titanite and $^{39}Ar/^{40}Ar$ ages show that the synkinematic intrusion of the Symvolon pluton was not later that 22–20 Ma (Dinter et al., 1995). Rb/Sr dating of biotite in the gneisses of the Pangeon-type unit in Thassos gives ages in the range 14–15 Ma that date deformation increments in the transition field of plastic-brittle mechanisms (Wawrzenitz & Krohe, 1998). This indicates that core complex-type exhumation of the Pangeon-type and Kerdylion-type units, controlled by the Kerdylion Detachment, ended in Langhian. Neogene sediments were deposited on top of the exhumed metamorphic rocks, within basins controlled by two sets of normal faults trending NE-SW and NW-SE. The oldest Neogene sediments are Serravalian in the Prinos basin (Kousparis, 1979) and Tortonian in most other basins (Karakitsios et al., 2017; Lalechos, 1986; Snel et al., 2006; Figures 2 and 4).

At regional scale, the layer-parallel foliation within core units dips dominantly at low angles (<20°) except close to the high-angle normal faults that separate the Neogene basins (e.g., Serres, Drama and Prinos) from the metamorphic and plutonic units of the surrounding mountains (e.g., Vrondou, Menikion, Falakron, and Pangeon) and Thassos island where steeper dips up to 50° are commonly observed (Figure 4b). The close relation between the bedding-foliation attitude, the present-day topography, and the high-angle fault pattern that affects Pangeon-type and Kerdylion-type units (Figure 4a) is a striking character of the SRCC indicating that (i) the present-day attitude of foliations as well as their trajectories at map scale (Figure 4b) and (ii) high altitudes (up to 2,000 m) do not mainly result from core complex syn-metamorphic deformation but from superposed Neogene normal faulting.

3.3.4. Thermochronology

Available low temperature ages (Figure 5) constrain the relative timing of core complex and Neogene basin development. The projection of all available ages on a line parallel to the mean direction of extension

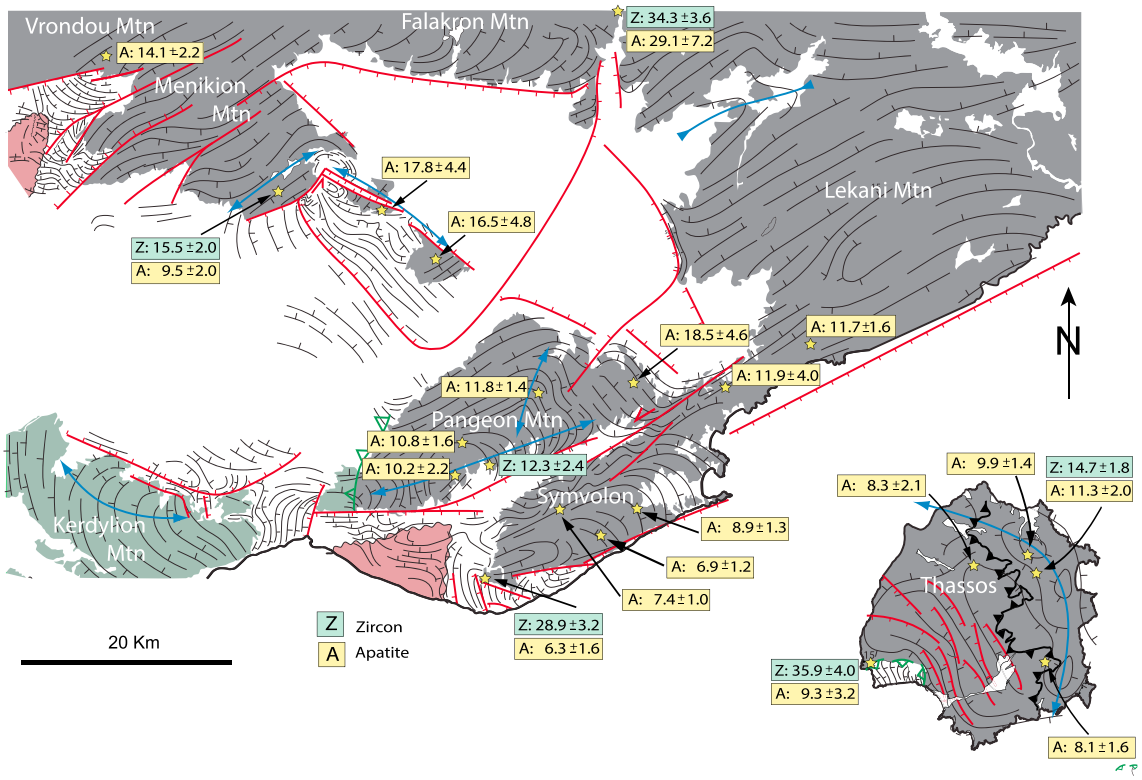

Figure 5. Location of available fission track (FT) dating in the studied area (green: zircon FT; yellow: apatite FT; modified after Wüthrich, 2009 and Kounov et al., 2015). Data from Bigazzi et al. (1994), Kyriakopoulos et al. (1996), Hejl et al. (1998), and Wüthrich, 2009). FT ages are reported as central ages (Galbraith & Laslett, 1993) ±2σ error.

(Kounov et al., 2015; Wüthrich, 2009; Figure 6a) shows that (i) the Kerdylion detachment started to accommodate extensional exhumation of the SRCC not later than 42 Ma, (ii) the extension end in Oligocene in the vicinity of the Nestos Thrust as shown by similar ages on the two sides of it, and (iii) all ages younger than 20 Ma are grouped in the central part of the profile where they are located the Neogene basins. The histogram of ages displays a double peak distribution (Figure 6b). The separation in three groups of apatite FT ages younger than 20 Ma, according the Neogene basin faults close to which they are located (Figure 6c), shows a systematic relation with the trend of normal faults that control Neogene basin deposition. Ages close to NW-SE trending normal faults are either the oldest (i.e., Drama Basin) or the youngest (i.e., Thassos), whereas those close to NE-SW trending normal faults (i.e., Pangeon and Prinos Basin) are intermediate. The Serravalian age of the oldest sediments in Prinos basin fits with the ages related to NE-SW trending faults. This timing pattern (Figure 6c) suggests that normal faulting could have started in the Drama area and migrated southeastward since 16–18 Ma (i.e., oldest ages close to the Drama basin but with large error bars of 4.6–4.8 Ma; Figure 5). These inferences from low-temperature dating will be further discussed in section 4 dedicated to the analysis of Neogene basins.

In summary, the timing of the SRCC development is bracketed by (i) the middle Eocene age of extension onset in the Northern Rhodope and along the Kerdylion Detachment and (ii) the later ductile deformation of gneisses in Thassos around 15 Ma and steep normal faulting and deposition of Neogene sedimentary basins, since at least Serravalian.

3.4. Significance of the Nestos Thrust and the Strymon Thrust

3.4.1. Nestos Thrust

The northern boundary of the SRCC (Figure 2), dipping at intermediate angle to the North, corresponds to a thrust-type contact between the "Rhodope Metamorphic Complex" (i.e., Northern Rhodopia) that contains ultrahigh pressure metamorphic rocks of Mesozoic age and the Pangeon-type unit of the Falakron and Lekani mountains (i.e., Pelagonia). This tectonic contact is often interpreted as a major thrust zone of

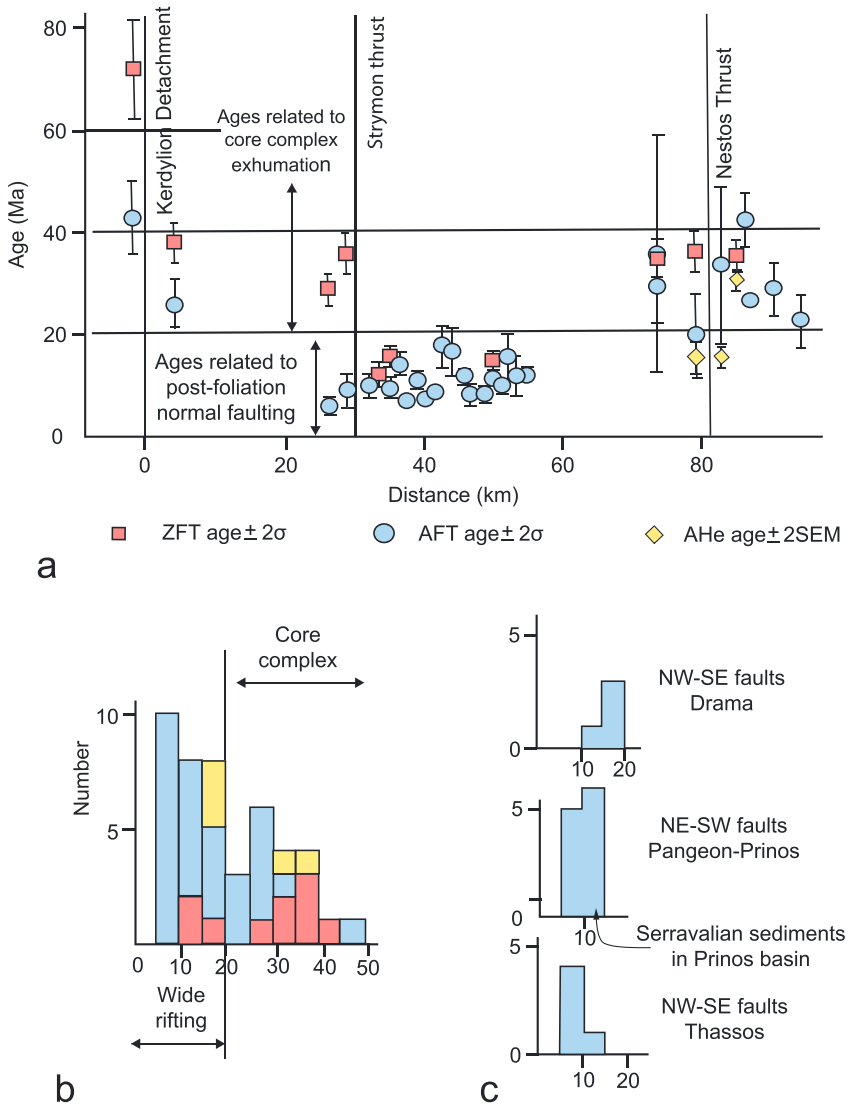

Figure 6. (a) Apatite and zircon fission track ages (AFT and ZFT) and five apatite [U-Th-(Sm)]/He ages (AHe; Kounov et al., 2015; Wüthrich, 2009) projected onto an SW-NE oriented profile (see location of data in Figure 5). (b) Histogram of age distribution. (c) Relation of AFT ages with trends of steep normal faults.

Alpine age as it put older on younger or more metamorphic on less metamorphic (e.g., Kilias & Mountrakis, 1990; Koukouvelas & Doutsos, 1990; Burg et al., 1996; see review in Burg, 2011). However, because the tectonic history of this contact is long and complicated, involving reactivation during the Tertiary, some authors call it in more neutral ways, for example, "Nestos Fault" by Dinter (1998) or "Nestos Shear Zone" by Nagel et al. (2011) or Gautier et al. (2017). Before SRCC exhumation the Southern and Northern Rhodopia (Figures 1a and 1c) constituted a single continental block below which Pelagonia has been subducted (Brun & Sokoutis, 2007; Kydonakis, Brun, Sokoutis, & Gueydan, 2015). Therefore, the Nestos Thrust was likely dipping at lower angle before Tertiary extension.

The Pangeon-type unit, located in the vicinity of The Nestos Thrust, and the base of the Rhodope Metamorphic Complex both display evidence of ductile deformation of late Eocene age (Bosse et al., 2009; Gautier et al., 2017; Nagel et al., 2011). However, both thrusting and extension have the same top-to-SW sense of shear leading to controversial interpretations. In particular, some authors have proposed that thrusting was active up to lower Oligocene and therefore that Tertiary extension in the SRCC could not be older than 27 Ma (e.g., Gautier et al., 2009).

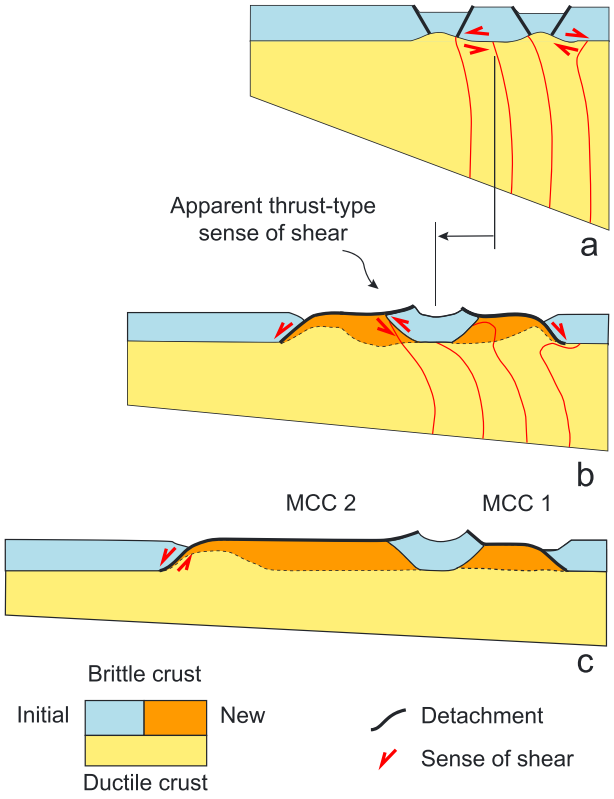

Figure 7. Diagram showing the development of core complexes in a spreading brittle ductile wedge (summarized from numerical models of Tirel et al. (2008) and analogue models of Kydonakis, Brun, & Sokoutis, 2015 see Figures 3a and 3b above).

The interaction between the NRCC and the SRCC during their exhumation explains the kinematics recorded along the Nestos Thrust. A three-stage diagram (Figure 7), inspired from thermomechanical (Tirel et al., 2008) and analogue (Kydonakis, Brun, & Sokoutis, 2015) modeling (see review in Brun et al., 2017) and adapted to the Rhodope example (i.e., extension of a thrust wedge), shows the processes involved and their kinematic implications. The three steps represented correspond to (i) early stage of extension and initiation of two core complexes MCC1 and MCC2 (Figure 7a), (ii) simultaneous growth of MCC1 and MCC2 (Figure 7b), and (iii) further growth of only MCC2 (Figure 7c). During the growth of a core complex, by a rolling hinge mechanism (Buck, 1988; Wernicke & Axen, 1988), the exhuming ductile crust progressively cools and becomes brittle below 350°C (taken as a proxy), as exemplified in thermomechanical models (Tirel et al., 2008; from pale to deep yellow in Figures 7b and 7c). Consequently, the "new" brittle crust fossilizes, through the closing temperatures of isotopic systems, the timing of core complex growth, and successive steps of ductile crust deformation prior to its cooling and not only those related to the detachment zone. During core complex growth, close to the detachment, the transient BD transition (i.e., prior to cooling) forms a domal structure whose apex is much shallower than in the backward part of the core complex previously exhumed (MCC 1 and 2 in Figure 7b; MCC 2 in Figure 7c). At the back of a core complex (side opposite to the detachment), the initial brittle crust undergoes an upward bending during ductile crust exhumation (Figure 7b). This effect brings the initial BD transition and the upper part of the ductile layer to the surface, allowing the direct observation of deformations that occurred in the ductile crust top during the previous stages of core complex development. The deformation of thin initially vertical red lines drawn in the ductile crust (Figures 7a and 7b) shows the horizontal shear below the initial brittle-ductile (BD) transition due to the growth of MCC 1 and simultaneous displacement of the block that separates MCC 1 and MCC 2. At the back of MCC 2, this sheared ductile crust is fossilized in the cooled ductile crust (Figure 7b) giving to the initial BD transition the appearance of a thrust.

To the north of the Nestos the NRCC domes (MCC 1 in Figure 7b), whose exhumation makes the Nestos Thrust footwall to reappear at surface, expose strongly deformed and partially molten gneisses (Burg, 2011; Gautier et al., 2017; Schenker et al., 2012) indicating that, during Tertiary extension, the crust underlying the Rhodope Metamorphic Complex was ductile. As mentioned above, the Nestos Thrust dip is not original but due to the upward bending of the brittle crust (i.e., hanging wall of the Nestos Thrust) during the development of the SRCC (MCC 2 in Figure 7b). Because the width of the NRCC domes in the direction of stretching is ranging between 30 and 50 km, the minimum displacement of the Nestos Thrust on top of the ductile crust must have been of at least 30 km, taking into account the upward bending of the Nestos Thrust. Therefore, the late Eocene age of SW-directed shear in the Nestos Thrust zone (Gautier et al., 2017) simply resulted from this rather large extensional displacement with top-to-SW sense of shear at the BD interface. In other terms, the Nestos shear zone that was the base of an Eocene age southwestward thrust wedge was still affected by a top to-SW sense of shear but extensional in late Eocene, as clearly identified by Nagel et al. (2011).

3.4.2. The Strymon Thrust

To the southwest end of the Pangeon mountain, the contact between Pangeon-type and Kerdylion-type units is a low-angle fault dipping southward that has been interpreted as a thrust (Kockel et al., 1977; Kockel & Walther, 1965) and is not a detachment as proposed by Dinter and Royden (1993), as it put older on younger. The same applies to the low-angle contact between gneisses and migmatites in the southwest of Thassos island (Brun & Sokoutis, 2007; for more details see Appendix A).

3.4.3. The Vardar Suture Zone Exhumed by the SRCC

As portrayed in Figure 1c, the SRCC can be viewed as Kerdylion-type and Pangeon-type units reaching the surface through a tectonic window opened in Rhodopia. In classical descriptions of Greece geology, the

Pangeon-type unit that is the dominant component of the SRCC is considered to be different from all other carbonate platforms lying on top a Hercynian basement (e.g., Figure 9 in Ricou et al., 1998; Figure 1 in Papanikolaou, 2013). However, the restoration of Aegean extension in map view and at lithosphere scale (Figures 9 and 10 in Brun et al., 2016) brings the Pelagonian domain, which largely outcrops in east continental Greece (Figure 1a), close to the Pangeon-type unit (Eocene in Figure 1b), suggesting that they likely belong to the same continental block that, consequently, we call "Pelagonia." This simplified way of portraying the geology of the Aegean domain presents the advantage of strengthening the tectonic importance the two suture zones of (i) Pindos between Adria and Pelagonia and (ii) of Vardar between Pelagonia and Rhodopia. According to this interpretation, we suggest here for the first time that the Strymon Thrust (i.e., the contact between the units of Kerdylion-type and the Pangeon-type; so-called Strymon Detachment) and the Nestos Thrust both correspond to the Vardar suture zone (Figures 1a and 1c). In addition, it is worth mentioning that in both South Pangeon and South Thassos, blocks of serpentinites outcrop along or close to this contact. The restoration of the regional scale cross section from southwestern Rhodope to Northern Rhodope (Figure 1c) illustrates the initial geometry of the Vardar suture zone within the thrust wedge prior to the onset of Aegean extension (Figure 1d).

4. Neogene Segmentation of the Southern Rhodope Core Complex

4.1. Method

For the study of the Neogene basins lying on top of the SRCC metamorphic rocks have been carried out using various existing data sources: (i) published stratigraphic data, low temperature dating of metamorphic rocks close to basins (Figures 5 and 6; (ii) 1/50.000 IGME geological maps; and (iii) seismic lines in the Prinos and Orfanos offshore basins (provided to us by J. Mascle). We carried out an extensive structural mapping of (i) the internal structure (bedding attitude and faults) of inverted and partially eroded basins and (ii) foliation trajectories in the metamorphic rocks along basin borders. This was completed by the structural analysis of fault patterns and décollement zones related to basin development in the metamorphic basement. We benefited from the expertise of G. Clauson and J-P Suc for the identification in the field of Messinian incisions and deposition of Pliocene Gilbert deltas of Akropotamos (between Pangeon and Symvolon) and Serres (between Vrondou and Menikion; Figure 3b; for details see Bache et al., 2011; Suc et al., 2015).

Three extensional systems are described separately in the following. Their distinction has been made in terms of (i) orientation and sense of dip of major normal faults and (ii) timing of development from available stratigraphic data and low-temperature dating (Figure 6c).

Using available geochronological data from metamorphic rocks, Brun and Sokoutis (2007); see their Figure 2) showed that a central band in the core complex, from Vrondou to Thassos, is characterized by ages younger than 15 Ma (i.e., Middle Miocene) that indicate cooling of core complex metamorphic rocks below 300°C. It is noticeable that this zone also corresponds to the location of the Neogene basins (Figure 2).

4.2. The Drama Extensional System

This extensional system corresponds to the fault pattern that accommodated the formation of the Drama Basin that is surrounded by the Falakron and Lekani mountains to the north and northeast and by the Menikion and Pangeon mountains to the southwest (Figure 4b). The basin has a diamond shape, a flat topography close to sea level, and its width reaches 20 km in its largest part (Figure 4a). Outcropping sedimentary units are Pliocene on borders and Pleistocene to recent Quaternary in middle. It is connected to the Strymon basin toward the southwest through the more than 20-km-wide Angitis basin between Menikion and Pangeon (Figure 4) in which bedding is generally very low dipping. The transition between Drama and Angitis basins occurs through a 6-km-wide rollover basin, the Alistrati rollover (Figure 4b), and not by a northeast-dipping normal fault as represented in most published maps of the area. A structural map showing the main faults and folds (Figure 8) and two interpretative cross sections (Figures 9 and 10) are used below to describe the Drama extensional system (Figure 8).

The Alistrati rollover was precisely mapped, thanks to a road cut located in its northwest end, almost perpendicular to the rollover trend (corresponding to section AA′ in Figure 8), and along which outcropping is nearly continuous. The Drama and Angitis basins being largely occupied by farming a lateral extend of bedding trends toward the southeast were obtained through interpolation of scattered outcrops. The rollover

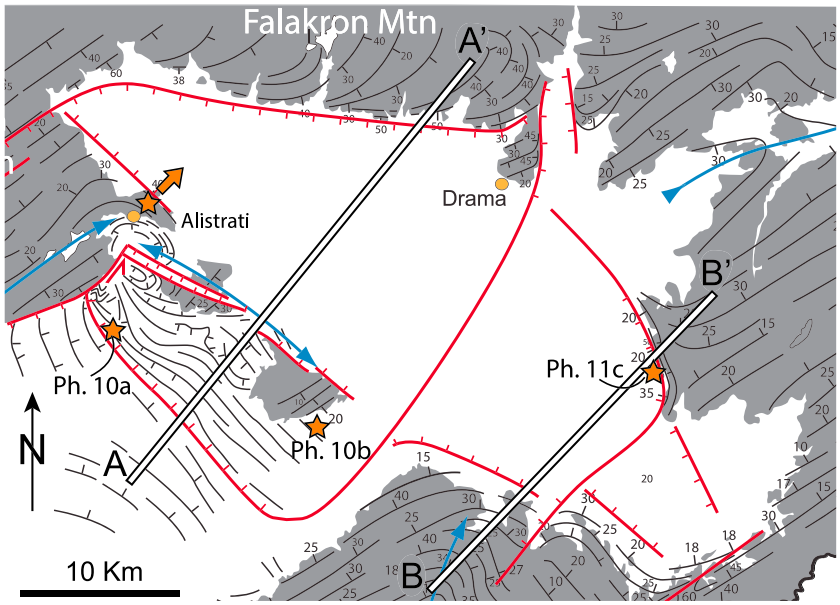

Figure 8. Structural map of the Drama extensional system with location of cross sections and photographs shown in Figures 10 and 11.

width, which is defined by an NE-dipping normal growth fault to the southwest and a rollover anticline to the northeast (Figures 8 and 9), increases along strike from 8 km to the northwest to 11 km to the southeast where it is covered by quaternary sediments. The growth fault position is defined, along the road cut, with a precision of 20–30 m but not directly observable. Close to the fault, sedimentary bedding is nearly horizontal in the footwall and dips around 50° in the hanging wall (Figures 9a and 9c). Within the rollover,

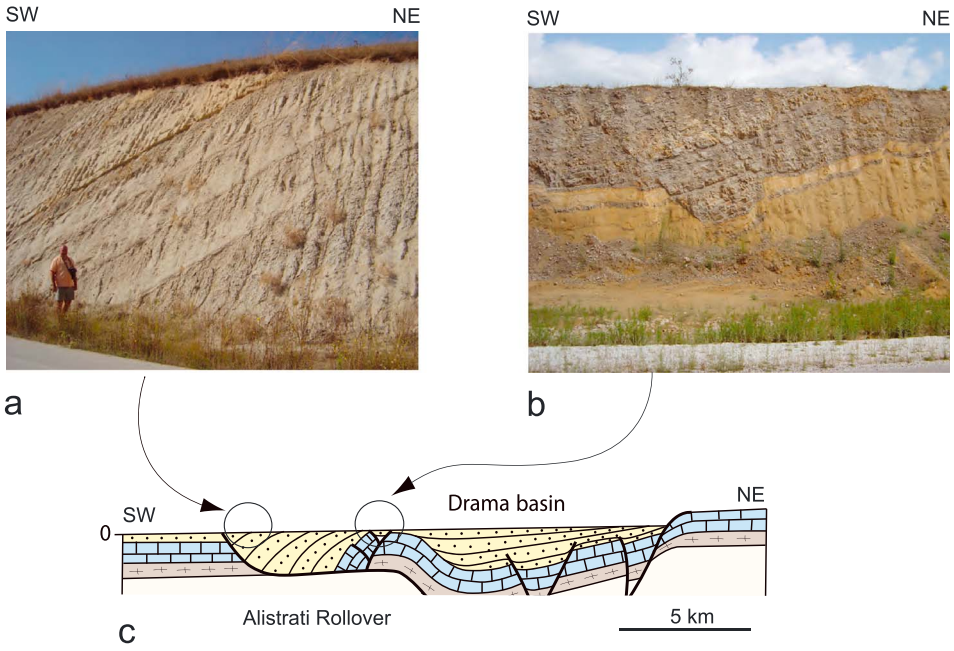

Figure 9. Photographs showing the 50° SW-dipping sediments close to the (a) growth fault of the Alistrati rollover and (b) conjugate normal faults in the rollover anticline close to the southwestern border of the Drama basin. (c) Interpretative cross section of the Alistrati rollover and the Drama basin. The fault pattern in the Drama basin is inspired from unpublished analogue experiments of ramp-flat experiments by the authors. For location of photographs see Figure 8.

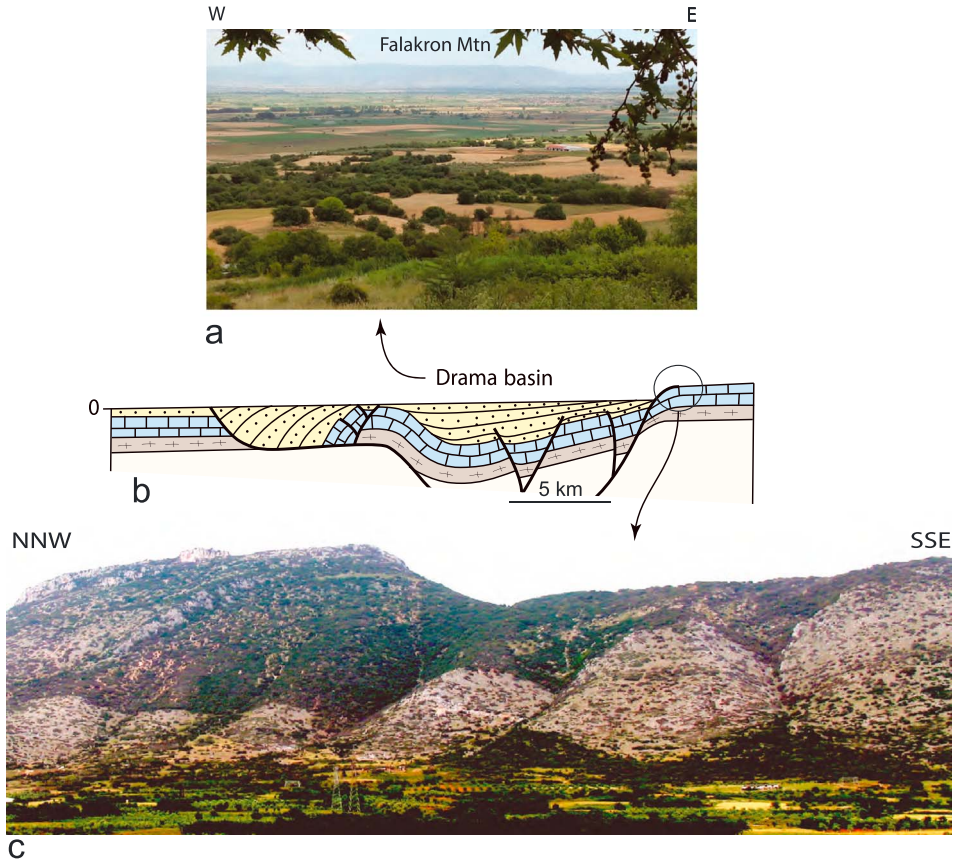

Figure 10. (a) Photographs showing the flat topography of the Drama basin and the high topography of the Falakron mountains (reaching 2,000 m) in the background and (b) the flexure of the Pangeon-type unit (marbles/pale above gneisses/dark) at the northern contact of the Drama basin. For location of photographs see Figure 8.

bedding dip remains in the range 40°–50° along most of the section and progressively decreases down to around 10° in the last 2 km before the rollover anticline axis, where sediments are deposited on top of a marble unit that outcrops in two erosional windows at map scale (Figure 8). Conjugate normal faults defining a graben type structure are located at the apex of the rollover anticline (Figures 8 and 9b and 9c). At Alistrati, the basal marbles in rollover anticline form a relief of around 50 m, above the Drama Basin flat surface (Figures 4a and 10a), that decreases progressively toward the southeast to become a smooth surface flexure where the basal marbles are covered by sediments affected by numerous conjugate normal faults (Figure 9b). Taking into account that the whole structure is significantly eroded, the rollover geometry indicates that the growth fault connects at depth of around 2 km with a subhorizontal décollement. The distance between the base of the growth fault and the anticline graben provides a proxy of 6 km for the horizontal displacement along section AA′ (Figure 9c).

The *northern limb of the Pangeon* does not show a structure directly comparable to the Alistrati rollover but a broad bending of the upper marble unit toward the southeastern part of the Drama Basin with a mean NE dip of 20°–30° (Figures 4b and 8). The marble layers dipping toward the Drama Basin are affected, from the top of the Pangeon mountain to the base, by extensional fractures nearly perpendicular to the foliation (Figure 11a), whose corresponding direction of stretching displays a constant NE-SW direction (Figure 11b). This brittle deformation likely formed when the marble layers were bent down the basin.

Along the *northern borders of the Drama basin* the metamorphic units of the Falakron and Lekani mountains display a downward bending or monocline folding (Figure 4). This is spectacularly illustrated at landscape-scale along the southern termination of the Lekani mountains (Figures 8 and 10c). Along this contact trending NE-SW, a thick marble layer lying on top of gneisses passes in a 2 km distance from horizontal to dips up

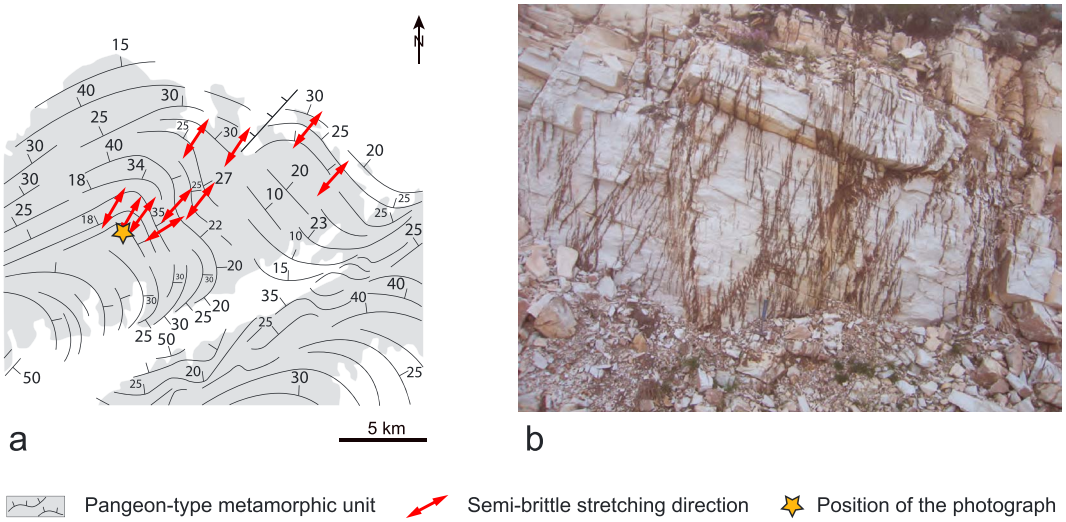

Figure 11. Extensional fractures nearly perpendicular to the foliation of marbles in the northeast flank of the Pangeon Mountain. (a) Stretching directions deduced from extensional fractures. (b) Photograph of the fracture pattern in marbles close to the Pangeon summit.

to 50° toward the basin. To the opposite side of the basin, the contact between the Falakron metamorphic rocks and the basin defines an E-W trending straight envelope over around 20 km (Figure 8). Foliation trajectories (i.e., envelopes of foliation trends) in marbles and gneisses are curved in a 2 to 3-km wide zone becoming southward parallel to the contact envelope, with basinward dips up to 50° (Figure 8). In the vicinity of the contact, 10 cm to meter scale normal faults or semibrittle shear zones and folds indicate a downdip sense of displacement (i.e., normal fault-type kinematics). This deformation pattern along basin contacts corresponds to a wide contact strain in the footwall of major normal faults (some 10 km long). Instead of being located into a narrow fault zone, deformation is distributed in a 2-km-wide zone in the footwall. It can be reasonably assumed that a similar contact strain could occur in the hanging wall hidden below basin sediments. The above observations indicate that the observed deformation occurred at a depth at which rheology of the metamorphic rocks is neither purely brittle nor ductile.

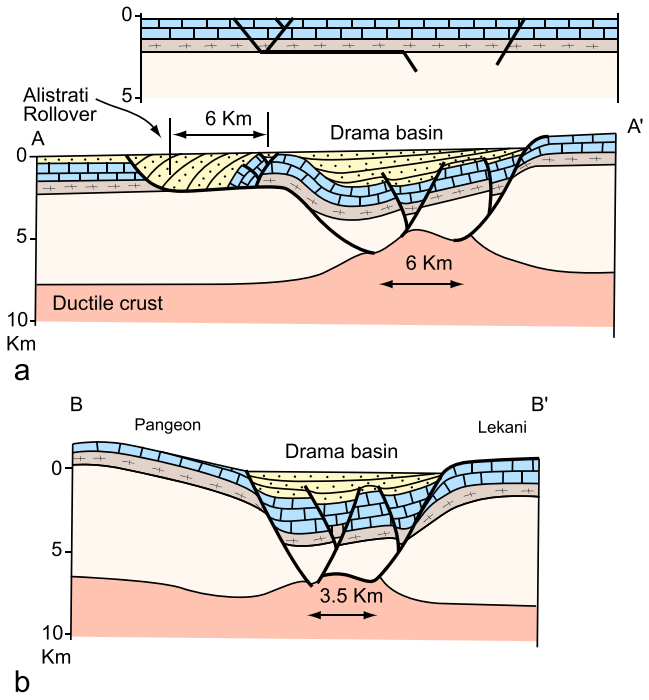

Figure 12. Interpretation of the Drama Basin structure at crustal-scale in the (a) northwestern and (b) southeastern parts of the Drama Basin. See location of sections in Figure 8. Fault pattern at depth inspired from unpublished analogue experiments of ramp-flat experiments by the authors.

4.2.1. Structural Interpretation at Crustal Scale

Two cross sections illustrate the interpretation at depth that can be proposed from the structures observed at surface (sections AA′ and BB′; Figure 8). In both sections (Figure 12), the structure of the Drama basin is a graben-type structure moderately asymmetrical. The depth and asymmetry of sedimentary fill in section BB′ is in agreement with geophysical imaging of a section close to our own by resistivity-magnetic model (Gurk et al., 2015). In section AA′ the southern graben normal fault is connected to the basal décollement of the Alistrati rollover.

The structures summarized above strongly suggest that the bulk diamond shape of the Drama basin results from the simultaneous opening of the two connected basins of South Falakron (SF) and South Lekani (SL). These basins display the following significant differences: (i) Their triangular shape likely results from a rotational opening, dextral for SF and sinistral for SL, with a mean radius larger for SF (35 km) than for SL (25 km); (ii) their maximum basin width is 20 km for SF and 16 km for SL; and (iii) their northern border fault is oriented E-W for SF and NW-SE for the SL. These differences imply that a transfer fault zone must have accommodated these differences during progressive graben opening.

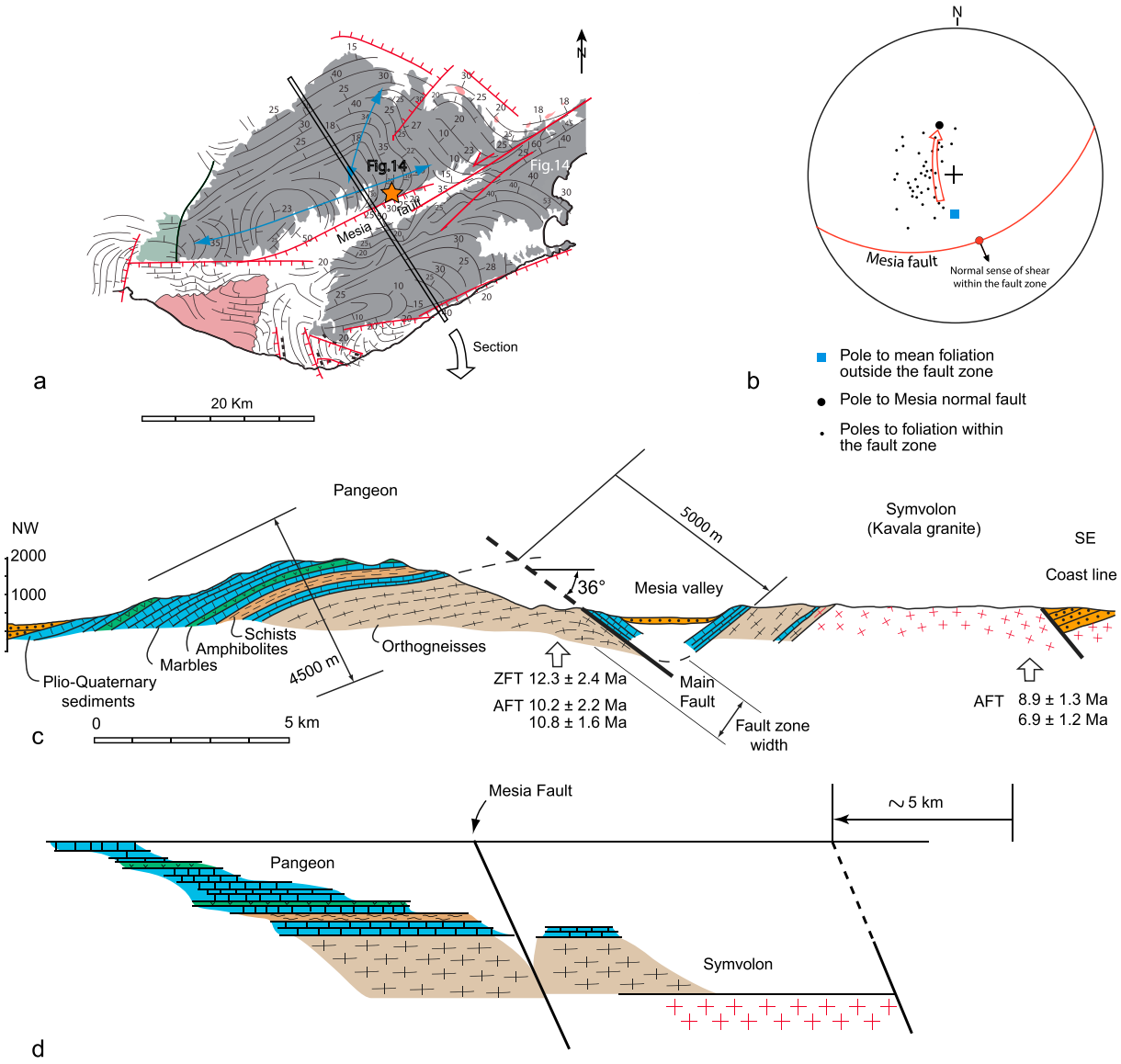

Figure 13. The Mesia fault and related tilting of the Pangeon and the Symvolon massifs. (a) Structural map with foliation trajectories and major faults. (b) Stereographic plot of foliation poles in the Mesia fault footwall. (c) Cross section (see location in a) showing the tilting of the Pangeon and Symvolon massives and dip and offset of Mesia fault. (d) Cross-section restoration and estimate of horizontal displacement with reference to the Pangeon.

All Drama Basin contacts with metamorphic rocks are characterized by wide zones (2–3 km) downward bending described above, except along the Alistrati rollover whose basal décollement connects at depth with the southern border fault of SF. This can happen when a low-angle weak zone is present within the upper crust (e.g., laboratory experiments by Nalpas & Brun, 1993). During its propagation toward the surface, the normal fault displacement is captured by the weak zone, which becomes a décollement giving a ramp-flat extensional pattern at upper crustal scale (Figure 12a). During graben opening, the layer lying on top of the décollement slips toward the graben. Passing above the intersection between décollement and normal fault, the layers bend down and slip on top of the normal fault footwall. The hanging wall basin becomes asymmetrical and synkinematic deposits acquire a fan-like structure (Figure 12a).

As already mentioned, most published maps and regional studies of the Drama area refer to an NE-dipping continuous normal fault that separates the Drama Basin from the Angitis Basin, from the northern border of the Menikion to the Pangeon mountain. In fact, such a fault does not exist. It is the Alistrati rollover anticline

that marks the boundary between the two basins (Figures 4 and 8). The only faults, observed close to Alistrati, are those resulting from outer-arc stretching in the rollover anticline (Figures 8 and 9b and 9c). From a mechanical point of view, the upper crust of the Alistrati rollover area must have involved a horizon weak enough to allow the development of a décollement. As illustrated in Thassos, duplications of marble and gneiss layers existing within the SRCC are due to Pelagonia subduction related thrusting prior to the onset of the SRCC and that a marble layer interlayered between thick gneiss layers was able to provide the condition for a décollement to developed (Brun & Sokoutis, 2007). Unfortunately, such observation is not possible in the crust underlying the Alistrati rollover, this area being low altitude and therefore without deep river incision and almost entirely covered by Angitis Basin sediments. Therefore, on the basis of Thassos observations, we hypothesize that similar thrust-related duplications of marbles and gneisses likely exist below the Angitis Basin and that the Alistrati rollover décollement is likely controlled by such a marble layer interlayered between gneisses.

4.2.2. Timing

Three low temperature ages (apatite FT), located two in the rollover anticline and one in the northern Pangeon limb, and ranging between 18.5 ± 4.5 Ma and 16.5 ± 4.8 Ma (Figure 5), indicate that faulting along the southern border of the Drama Basin started between late early Miocene and middle Miocene. However, note that error bars are so large that faulting could be Langhian-Serravalian or close to.

4.3. The Mesia Fault and Pangeon Block Tilting

4.3.1. The Mesia Fault

The Pangeon mountain is separated from the Symvolon mountain by the narrow and 20-km-long Mesia valley (Figure 4) whose location and morphology are strongly controlled by a major normal fault, described here for the first time and that we name "Mesia Fault" (MF; Figure 13). The NW flank of the Pangeon mountain corresponds dominantly to the marble cover lying on top of basement gneisses that largely outcrop in its SE flank, along the Mesia Valley. Marble foliation in the NW flank has a mean dip of 30° toward the NW and trends nearly parallel to the MF showing that the Pangeon mountain is a large tilted block, 30 km long and 14 km wide (map and cross section in Figures 13a and 13c, respectively). In the eastern part of Mesia Valley, where the fault trace can be located precisely, mean fault dip is 36° ± 3°. Taking the interface between the marbles and orthogneisses as reference in both Pangeon and Symvolon, a mean dip-slip offset of 5 km can be estimated for the MF.

4.3.2. Semibrittle Deformation in the Mesia Fault Zone

The MF, like the faults surrounding the Drama Basin, displays a distributed deformation in the footwall (i.e., Pangeon metamorphic rocks) as demonstrated by the curvature of foliation trajectories in the gneisses close to the MF (Figure 13a). A stereoplot of foliation poles in this zone of trajectory curvature shows a continuous dispersion from the mean foliation pole in NW flank (bleu square in Figure 13b) toward the MF pole (red dot in Figure 13b). This indicates that gneiss foliation, whatever its initial strike and dip, is sheared toward parallelism with the MF.

In strongly banded mylonitic gneisses of the Pangeon that outcrop close to the MF, various decimeter- to meter-scale structures illustrate a semibrittle behavior during normal faulting (e.g., faults, breccias, flexural folds, and ramp-flat structures). Among the most spectacular are the extensional ramp-flat displacement surfaces. In the example shown in Figure 14, foliation envelopes are underlined in blue and red to separate the hanging wall and footwall, respectively. A footwall ramp to the left (red) and a hanging wall ramp (blue) are identified where the low-angle fault intersects the foliation of mylonitic gneisses. The layer colored in yellow that is rich in micas played the role of a décollement. During displacement, the hanging wall ramp rotated downward (i.e., rollover) against the décollement layer and the footwall ramp was rotated upward (i.e., rollunder). This structure cannot be confused with any shear structure that would have developed during previous ductile deformation (i.e., core complex exhumation) as its displacement is nearly perpendicular to the stretching lineation and shear bands associated to high-temperature mylonites. This deformation pattern that is neither entirely brittle nor entirely ductile, called here "semibrittle," is typical of the one that accommodated the reorientation of the preexisting foliation-layering of metamorphic rocks toward the MF. As indicated by the estimated offset of the MF, it likely developed at a depth of around 4–5 km. Fission track data in the MF footwall (Zircon FT: 12.3 ± 2.4 Ma; Figure 5), where these semibrittle structures are observed, indicate that temperature was close to 300°C in Serravalian at the onset of faulting, not far above the BD transition, if we take 350°C as a proxy for BD-transition in rocks of granitic composition.

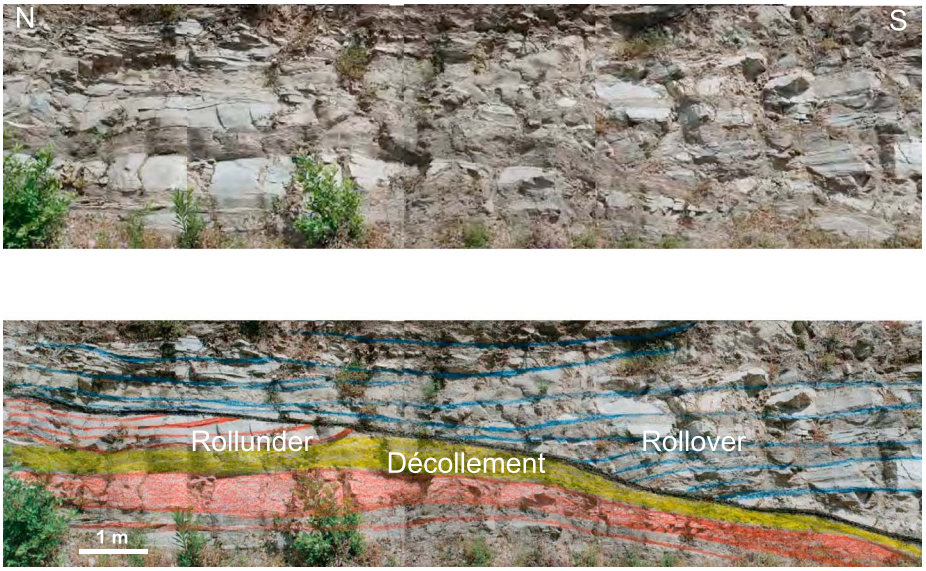

Figure 14. Mylonite and ultramylonitic banding affected by a meter-scale ramp-flat extensional structure in the Mesia fault footwall. Photographs (a) noninterpreted and (b) interpreted.

4.3.3. The Pangeon and Symvolon Tilted Blocs

A rotation back to horizontal of the Pangeon marble pile, around a horizontal axis, restores the MF to an original dip of 65° ± 6°, similar to most normal fault dips at initiation, what validates the tilted block interpretation. The restoration of the Pangeon and Symvolon blocks (Figure 13d) shows that (i) block tilting has accommodated a displacement of around 5 km toward the southeast of the Symvolon block and (ii) the Pangeon has undergone a mean erosion of 1.3 km and the Symvolon is even more deeply eroded (i.e., $>$4 km). Such large amounts of erosion, in spite of still high altitudes (Pangeon peak at 2,000 m), imply that erosion has been active during block tilting.

4.3.4. Timing

Four apatite FT ages located in the footwall gneisses of the southeastern flank of the Pangeon and ranging between 12.3 ± 2.4 Ma and 10.2 ± 2.2 Ma (Figure 5) indicate that the MF that accommodated Pangeon block tilting was active in middle Miocene (i.e., Serravalian-Tortonian). Four apatite FT ages located in the Symvolon block ranging between 8.9 ± 1.3 Ma and 6.3 ± 1.6 Ma (Figure 5) indicate that the normal fault parallel to the coast line of the Prinos Basin (Figure 2) was active in late Miocene (i.e., Tortonian-Messinian) but with an important contribution of erosion as mentioned in the previous section, especially in the Symvolon. As a whole, these ages are in good agreement with the ages of first sediments deposited in the Prinos Basin, Serravalian in its northern part (Kousparis, 1979), and Tortonian between Symvolon and Thassos (Proedrou & Papaconstantinou, 2004).

4.3.5. Horizontal Displacements During Basin Development

Using the estimates of horizontal displacement, accommodated by the Drama extensional system and the Pangeon-Symvolon block tilting, we attempted to reconstruct the initial geometry of the fault pattern at regional scale (Figure 15). This restoration shows that during core complex segmentation by normal and strike-slip faults the Kerdylion massif was displaced southwestward of around 18 km with reference to the northern part of the core complex.

4.4. The "Thassos-Orfanos" Extensional System

The *Thassos Island* (Figures 2 and 4) exemplifies in an area of a rather limited extend (25 km in the direction of extension): (i) the duplication by thrusting of the Pangeon-type unit, (ii) the thrust contact between Pangeon-type unit and Kerdylion-type unit, (iii) ductile deformation related to core complex extension, and (iv) normal faulting and deposition of the Neogene Limenaria Basin (Brun & Sokoutis, 2007; Figure 16). The present section focuses on extensional faulting and kinematics of basin deposition during Neogene.

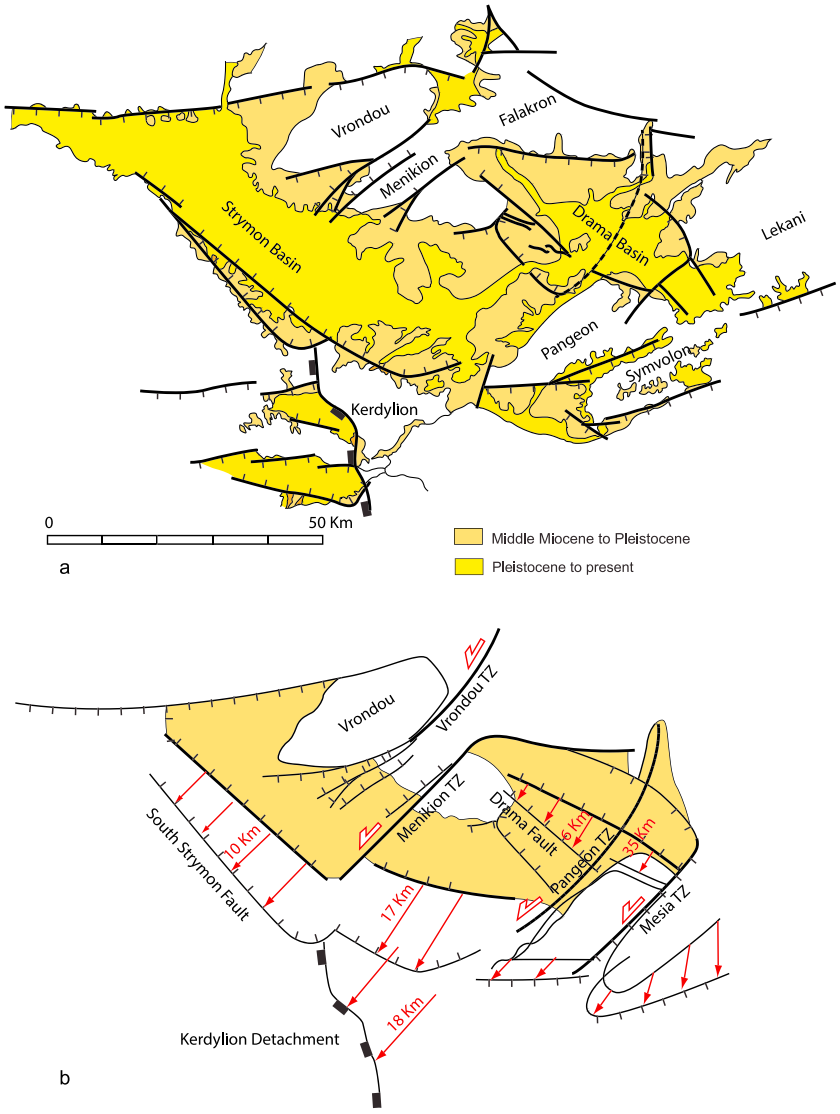

Figure 15. Neogene basins from Drama to Strymon. (a) Map of present-day contours. (b) Restored geometry in middle Miocene, at the onset of steep normal faulting.

The general structure of the Thassos island can be described in simplified way in two main parts (Figure 16): (i) a large anticline located to the northeast with a slightly curved axis trending as a mean NNW-SSE and (ii) a broad monocline dipping at low angle in an SW direction, almost perpendicular to the anticline. The anticline core (green in Figure 16) is made of a thick pile of marbles and schists, corresponding to the lower unit. On top of the southwest anticline limb, separated by a thrust from the lower unit, is the middle unit (red in Figure 16) made of marbles lying on top of Hercynian gneisses (i.e., Pangeon-type unit). The upper unit (i.e., Kerdylion-type unit; dark gray in Figure 16) outcrops at few restricted places along the Limenaria Basin contours, to the southwest of the island. The upper unit-middle unit contact corresponds to the Strymon Thrust (see section 3.4).

4.4.1. Limenaria Basin

Sediments of the Limenaria Basin outcrop along the southwestern coastline of Thassos over around 15 km (Figure 16). The largest outcrop, located to the north of the basin, offers a continuous cross section, perpendicular to the main bedding trend, along 6 km, from Scala Maries to Limenaria. The other smaller basin remnants allow an interpolation that shows the constant NNW-SSE bedding trend at island scale and that also

Figure 16. Simplified geological map of Thassos Island showing the three metamorphic units, the Limenaria basin, and the main basin-related structures (thrust faults, normal faults, anticlines, and transfer zones). Note the difference in trend of stretching lineations in the lower unit (green) and the middle unit (red). In the lower unit, lineations trend perpendicular to bedding orientation in the Limenaria basin. The large green arrows indicate the displacement of middle unit on top of lower unit.

offers several well-exposed sites of the basal basin contact. With the exception of the northern border of the basin, the bedding displays a very constant dip of 30° to the ENE (Figures 17b and 17d). The basin is intracontinental mainly filled with conglomerates with one interval of fine-grained clastics (Figure 17b) and one interval of large olistoliths close to Limenaria. At 1–2 km west of Limenaria, two sites have been dated with pollens as late Pliocene and early Pleistocene (Lyberis & Sauvage, 1985), suggesting that the oldest layers exposed along this section of the Limenaria Basin could be late Miocene to early Pliocene.

Detailed mapping along the 6 km long and continuous section does not reveal the existence of any major normal fault within the basin. The largest observed fault offsets do not exceed few meters. This means that the regular 25–30° dip of the beds toward the ENE does not result from block tilting but represents a rollover-type geometry with a minimum amplitude of 6 km. The normal faults belong to two main families: one subvertical and the other dipping around 30° to the WSW. The bisector of the acute angle between the two fault families is perpendicular to bedding indicating (i) that faulting started while the layers were still nearly horizontal and (ii) that they rotated of a mean 30° angle toward the ENE, together with bedding during rollover growth.

At map scale, the sediments are lying on top of middle unit marbles with few remnant blocks of the upper unit made of serpentinites and migmatitic gneisses dated around 50 Ma (Wawrzenitz & Krohe, 1998; Figure 16). The contact between upper unit and middle unit is a thrust (i.e., Strymon Thrust; see section 3.4) that puts gneisses and migmatites of the Kerdylion-type unit on top of marbles of the Pangeon-type unit (Figure 4b). Where the contact of the sediments with the metamorphic rocks is best observed, the underlying marbles are finely brecciated and dolomitized over 2 m maximum below the contact. The brecciated marble surface that dips regularly 6° to the WSW is corrugated with crude striaes trending dip parallel. Conglomerates display meter-scale shear bands in the 2 m above the contact, but bedding dip still remains around 30° without evidence of strong penetrative deformation close to the contact. The above structural observations demonstrate that this contact cannot be considered as a core-complex detachment, as proposed by Wawrzenitz and Krohe (1998).

4.4.2. The Ramp-Flat Extensional System of Thassos

To the northeast of the basin contact, marbles and underlying orthogneisses are affected by steeply dipping normal faults (Figure 17c), trending parallel or slightly oblique to the strike of the basin sediments (Figure 16) showing that they were part of the brittle crust at the time of sediment deposition. Lateral variation in the location and spacing of normal faults define at map scale transfer zones trending in a mean NE-SW direction (Figure 16). At the northern end of the Limenaria Basin, close to Scala Maries, one of these transfer zones displays upright folds and thrust faults in the middle unit marbles (Figure 17a).

The marbles underlying the middle unit gneisses, which appear within few km-wide windows of the middle unit and in the northeastern anticline (Figure 16), acted as a décollement below the faulted middle unit. Mineralogical and geochemical analyses of hydrothermal deposits along and around large steep faults of the middle unit reveal that the décollement was likely accompanied by fluid circulation at temperatures in the range 100–200°C (Boulvais et al., 2007). Textural and microstructural patterns show that strain localization at the top of lower unit marbles was linked to decreasing pressure-temperature conditions and Solvus thermometry, indicating that temperatures of 300–350°C prevailed during part of the shear deformation history (Bestmann et al., 2000).

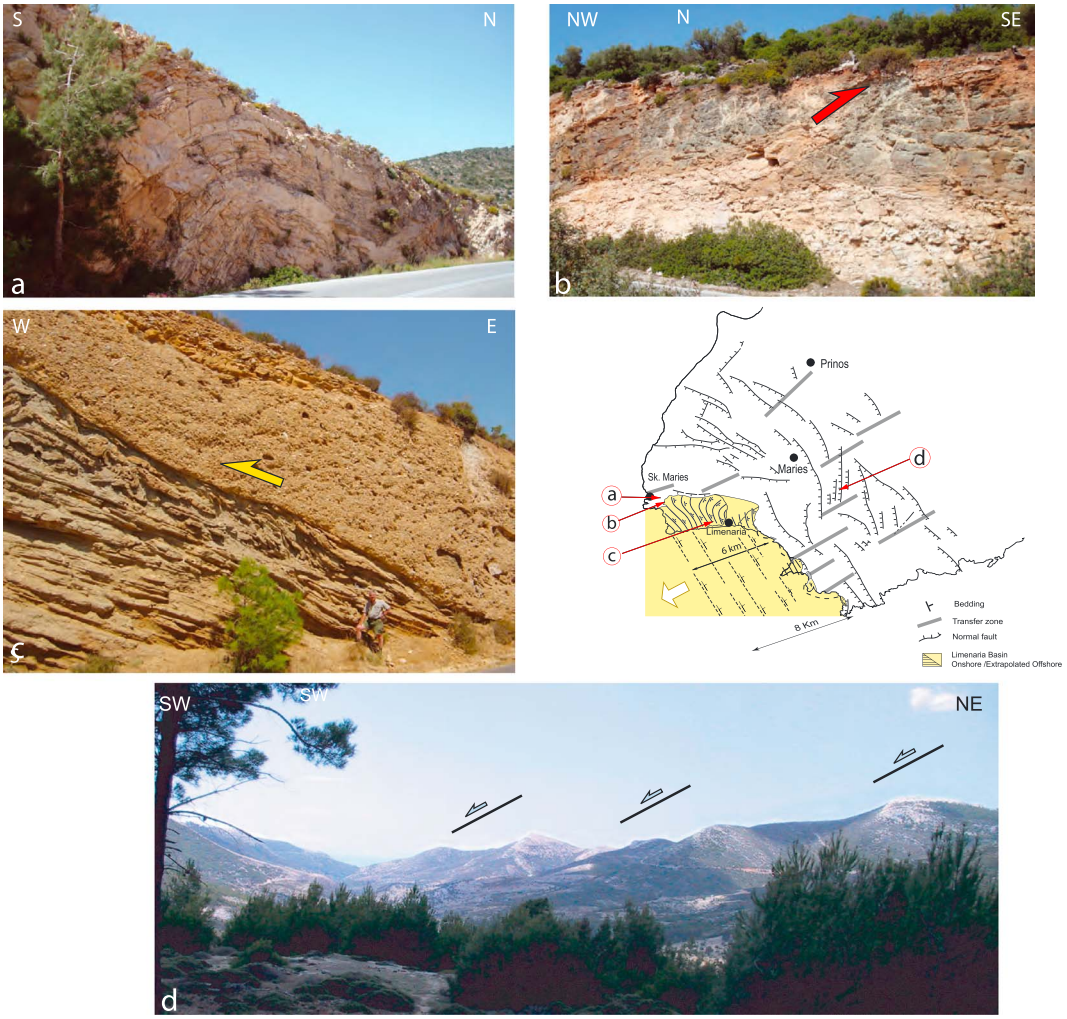

Figure 17. Some characteristic structures in and around the Limenaria basin. (a) Upright folds and (b) thrust fault in marbles and amphibolites close to the Maries transfer fault. (c) Fine grain sediments and conglomerates close to Limenaria. Layers of fine grain sediments were folded during the mass-flow emplacement of conglomerates (indicated by yellow arrow) and later tilted at an angle of 25° during rollover displacement toward the west southwest. (d) Panorama looking toward the SW showing a series of tilted blocks affecting marbles (pale) on top of gneisses (dark) in middle unit.

The pattern of folding and faulting at island scale and its relation with the Limenaria basin internal structure (Figure 16) indicates that Neogene deformation that controlled the deposition of the Limenaria Basin corresponds to a ramp-flat extensional system as illustrated in three steps in Figure 18b. This extensional system is composed of a merging ramp located to the northeast and a blind ramp located to the southwest connected by a décollement within the marbles of the lower unit. Localized extension along the merging ramp accommodated the rise of the lower unit forming the northeastern anticline. Simultaneously, the southwestward middle unit displacement was accommodated by layer-parallel shear in the underlying middle unit marbles. In passing above the southwest blind ramp, the middle unit underwent a downward bending responsible for a syncline folding of the middle unit in which Neogene sediments were deposited. The sediments deposited horizontally near the ramp were tilted by 30° during displacement, forming a piggyback rollover basin. The constant layer dip of 30° toward the NE in the rollover implies that the blind ramp is also dipping by 30° but toward the SW. During displacement, the décollement layer thinned and the overlying middle unit underwent faulting and block tilting between the eastern anticline and the basin. A direct implication of such a flat-ramp-type extension is that the basin width provides a direct estimate of the minimum amount of displacement—that is, around 8 km for the Limenaria basin (Figure 16). Over around 5 km to the northeast of

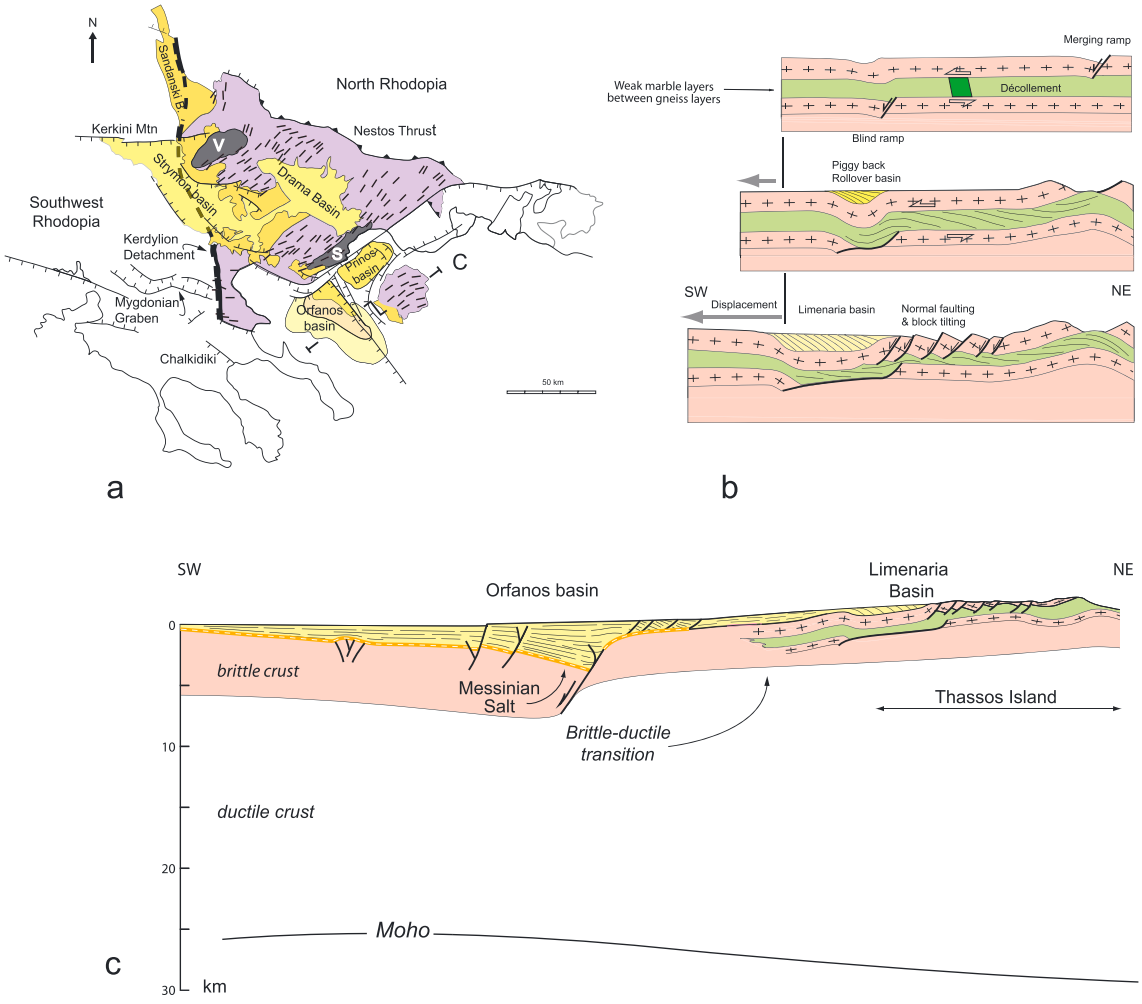

Figure 18. (a) Map scale relation between the onshore Limenaria basin of Thassos and the Orfanos offshore basin. (b) Three-step sketch illustrating the initiation and amplification of the ramp-flat extensional system of Thassos and the rollover growth of the Limenaria basin. (c) Crustal-scale cross section showing the geometrical relation between Limenaria and the Orfanos basins (see location in a).

the Limenaria Basin border, middle unit blocks are tilted from 25° to 30° (see structural map [Figure 10] in Brun & Sokoutis, 2007). Block tilting (α) and horizontal stretching ($1 + e_h$) are related by the two following equations: $(1 + e_h) = \sin p_0/\sin p$ and $\alpha = p_0 - p$, where p_0 and p are the initial and final normal fault dip (Brun & Choukroune, 1983). These relations indicate that the tilted block zone located at the back of Limenaria Basin has accommodated from 50 to 70% of horizontal stretching meaning that the final 5 km width of this zone resulted from 1.6 to 2.0 km of horizontal elongation. From the above estimates, it can be concluded that a minimum bulk displacement of around 10 km has been accommodated by ramp-flat extension in Thassos.

4.4.3. Timing

Within the northeastern anticline, Rb-Sr isochron ages of biotite are 13.3 ± 0.1 and 12.0 ± 0.1 Ma (i.e., Serravalian) reflect cooling of high-temperature mylonites of the lower unit below approximately 300°C (Wawrzenitz & Krohe, 1998). Among the five apatite FT ages available in Thassos (Figure 5), two are located in the lower unit (9.9 ± 1.4 Ma and 11.3 ± 2.0 Ma), two in the middle unit (8.3 ± 2.1 Ma and 8.1 ± 1.6 Ma), and one in the upper unit (9.3 ± 3.2 Ma), indicating that cooling below 110° occurred from Tortonian to early Messinian. The above ages indicate that the ramp-flat extensional system of Thassos initiated in Serravalian and the youngest ages of sediments in the Limenaria rollover basin (Lyberis & Sauvage, 1985) that extensional displacement continued up to late Pliocene-early Pleistocene.

4.4.4. Relation With the Orfanos Basin

The Orfanos Basin, as documented by industry seismic lines (Mascle & Martin, 1990), is a large basin with more than 3,000-m-thick depocenter above the Messinian salt (i.e., Pliocene to Quaternary; Figure 18c) and therefore largely of the same stratigraphic range of that of the Limenaria Basin. Its asymmetrical structure is controlled by a major SW-dipping normal fault to which the Thassos décollement is likely connected defining a ramp-flat structure at upper crustal scale.

5. Discussion and Conclusions

5.1. The Two-Stage Evolution of the Southern Rhodope Core Complex

The evolution of the SRCC, during the Hellenic slab rollback (Figure 1b), occurred in two main stages, first core complex-type extension and then segmentation of the core complex by distributed steep normal faults and deposition of Neogene basins (i.e., wide rift-type extension). The transition between the two stages occurred in middle Miocene is constrained by the Serravalian age of oldest sediments in basins and (ii) Rb-Sr isochron ages of biotite (14–15 Ma) that reflect cooling during Langhian of high-temperature granite mylonites below approximately 300°C (Wawrzenitz & Krohe, 1998).

A two-steps restoration since Eocene of the initial geometry of the main geological units summarizes this evolution in map view at the scale of the northern continental Greece (Figure 19). During Eocene, two extensional zones initiated within the upper crust of Rhodopia (Figure 19a) whose evolution up to middle Miocene gave the two core complex domains the NRCC in Bulgaria and the SRCC in Northern Greece (Figure 19b). Since middle Miocene, the southern part of the SRCC was segmented by normal faults trending NW-SE and NE-SW that controlled the deposition of Neogene basins (Figure 19c).

The second stage, since middle Miocene, represents a large-scale event as it occurred at whole Aegean scale and not only in areas where the first stage was characterized by the exhumation of metamorphic rocks, either of high temperature (i.e., core complexes in Rhodope and central Cyclades) or high pressure (i.e., blueschist belts of the Cyclades and Peloponnese-Crete; Brun et al., 2016). In the Rhodope, the contact of Neogene sediments with underlying metamorphic rocks is either depositional or corresponds to steep normal faults. Nowhere basin base corresponds to a major detachment what puts seriously in question the so-called "Strymon detachment" (see Appendix A).

The segmentation of a core complex by steep normal faulting and basin deposition, as documented in the Rhodope, has several important mechanical and geological implications that deserve more detailed discussion. From a mechanical point of view, four aspects are of particular interest: (i) the ramp-flat extensional systems, (ii) the location of basins to the SW of the SRCC, (iii) the widening of basins from NW to SE, and (iv) the transition from core complex exhumation to basin development (i.e., segmentation of the core complex).

5.2. Deposition of Neogene Basins Above an Extending Hot Crust

5.2.1. Ramp-Flat Extensional Systems

The ramp-flat patterns of extension leading to rollover basin geometry that we documented in Alistrati (Drama extensional system; Figures 8 and 9) and in Limenaria (Thassos-Orfanos extensional system; Figure 18) have strong implications in terms of upper crust rheology. A ramp-flat geometry of extension is obtained when displacement along steeply dipping normal faults located at different levels is transferred along a shallow dipping horizon (i.e., décollement). This implies that the décollement layer is significantly weaker than the overlying and underlying layers. In Thassos, marble layers interlayered between gneiss layers by early thrusting underwent ductile deformation during basin development, providing such suitable décollement layers at temperatures in the range 100°C–300°C in presence of fluids (Bestmann et al., 2000; Boulvais et al., 2007). In both examples described above the depth of the décollement layer was in a depth range of 2–3 km indicating very high temperature gradients. In a dominantly gneissic crust with a BD transition at a proxy of 350°C, the upper brittle crust cannot have been thicker than 7 km, giving a minimum geothermal gradient of 50°C/km. *Such a thin upper brittle crust implies that the crust was hot at the place and time of basin development*. This is in agreement with the semibrittle behavior of mylonitic gneisses in the footwall of the MF (Figure 14) that were seated at 5 km depth at onset of faulting (Figure 13). A semibrittle behavior is also observed along the northern borders of the Drama basin where it has accommodated a 2 to 3-km-wide downward bending of gneisses and marbles (Figures 8 and 10c).

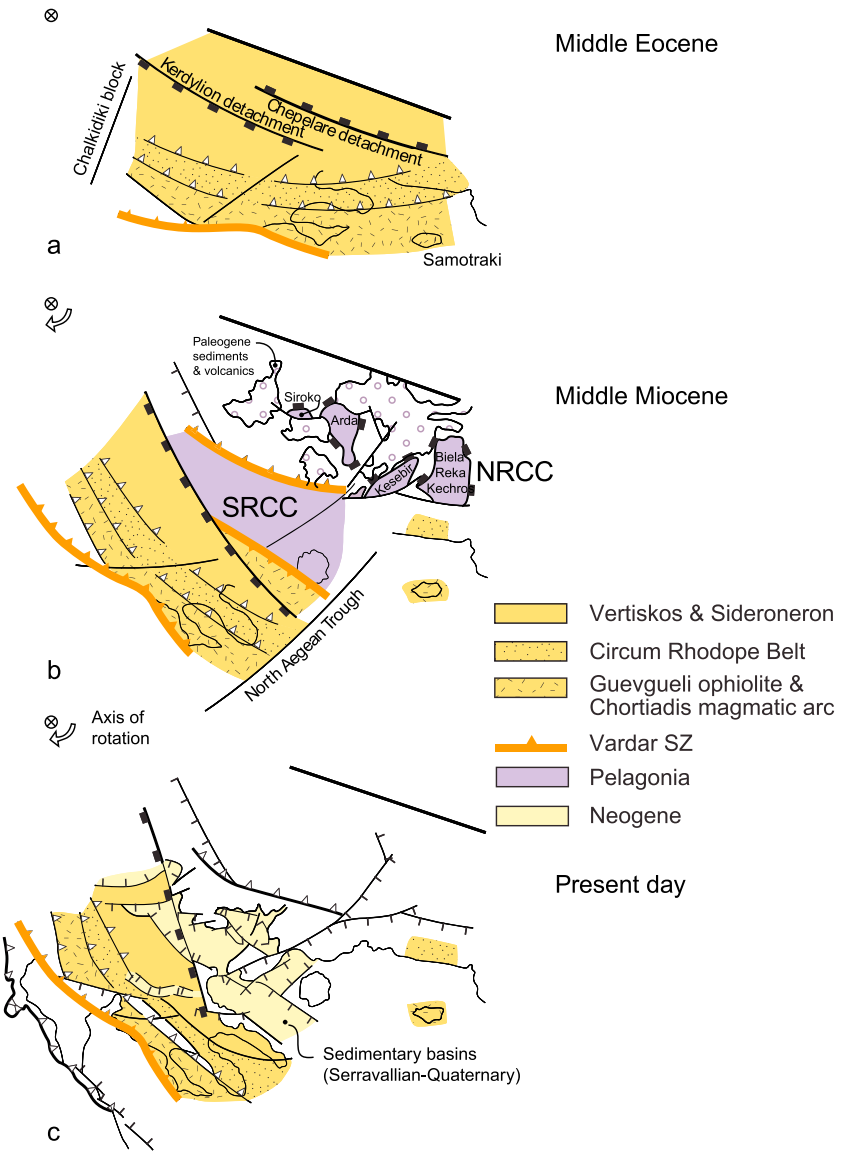

Figure 19. The two-stage tectonic evolution of the Rhodope accommodated by a 30° rotation of the Chalkidiki block with the units of Guevgueli ophiolite-Chortiadis magmatic arc and Circum Rhodope Belt identified to underline the evolution. (a) Initial geometry in middle Eocene of the Rhodope at the onset of core complex extension and initiation of the Chepelare and Kerdylion detachments. For clarity, only the structures that developed during each stage are represented in b and c. (b) End of stage 1 in middle Miocene: Geometry of Northern and Southern Rhodope Core Complexes (NRCC and SRCC). (c) Present-day geometry resulting from stage 2 since middle Miocene: wide rift segmentation of the Southern Rhodope Core Complex by steep normal faults and deposition of Neogene basins.

5.2.2. Basin Location

The basins are located close to the Kerdylion detachment (Figures 2 and 19c). Thermomechanical modeling shows that core complex results from a localized mode of extension (see Figure 11 in Brun et al., 2017). In a two-layer BD model core complexes develop after an initial graben whose enlargement allows the initially ductile crust to reach the surface (as sketched in Figure 7). Approaching surface, the ductile crust cools and becomes brittle. Consequently, in an actually exhuming core complex, the brittle layer is thinner close to the detachment than away from it where longer time of cooling has built a thicker brittle layer (Figures 7b and 7c). This strongly suggests that *the shallower depth of the BD transition close to the detachment has controlled basin location at the time of their onset*, as the strength of the brittle crust directly depends on

its thickness. This is in agreement with a hot crust at the place and time of basin development deduced from the formation of ramp-flat extensional systems where marble units are interlayered with gneiss units (see previous section).

5.2.3. Effect of Block Rotation

During Tertiary extension and progressive exhumation of the SRCC a differential clockwise rotation occurred between Northern Rhodope and Chalkidiki block as documented by paleomagnetism (Dimitriadis et al., 1998). Brun and Sokoutis (2007) argue that this block rotation at regional scale was responsible for (i) the wedge shape of the SRCC in map view and (ii) the curvature of stretching lineations inside the core complex. In such a rotational pattern of extension the amount of stretching increases with the radius explaining why the basins widen from NW to SE (Figure 2) away from the pole of rotation (Figure 19). The fact that both core complex exhumation and basin development have both recorded effects of block rotation would confirm if necessary that they both represent continuity in extension rather that superposed and distinct phases of deformation.

5.3. The Transition From Core Complex to Wide Rifting as Due to an Increase of Stretching Rate

Mean stretching rates for the two modes of extension (i.e., core complex and steep normal faulting) can be estimated as follows.

For the *core complex stage*, the amount of displacement Δl is given by the core complex width (120 km along the Aegean coast line; Brun & Sokoutis, 2007) minus the displacement related to the basin development (around 20 km along the Aegean coast line; Figure 15). Taking 42 Ma, youngest possible age of the Kerdylion Detachment, and 13 Ma, age of the transition to steep normal faulting, the duration Δt of core complex extension is around 29 Myr. This gives a mean velocity of displacement of 0.3 cm/yr.

For the *basin stage*, the amount of displacement $\Delta l = 18$ km is obtained from the restoration of the basin area from Drama to Strymon (Figure 15). The duration Δt of basin extension is estimated around 13 Ma age of the transition between the two stages of extension minus 1 Myr, roughly the time at which the stretching direction changed from NE-SW to NS in the whole North Greece (as quoted in section 5.1). This gives a mean velocity of displacement of 1.5 cm/yr.

The above estimates for the two stages of SRCC evolution indicate that the mean velocity of displacement increased by a factor 5 from core complex to steep normal faulting and, consequently, to a segmentation of the core complex. This directly compares with the acceleration of the velocity of trench retreat at whole Aegean scale also by a factor 5, from 0.6 cm/yr during the first 30 Myr of slab rollback, characterized by the exhumation of metamorphic rocks accommodated by detachments, to up to 3.2 cm/yr during the last 15 Myr (see Figure 11 in Brun et al., 2016). The widespread distribution and simultaneous development of Neogene basins at Aegean scale, over around 1,000 km from north to south, show that the second stage of extension observed in the Southern Rhodope corresponds to a wide rift-type mode (Buck, 1991) of crustal extension. From a mechanical point of view, the change of extension mode, from core complex to wide rift, corresponds to an increase in coupling between the brittle and ductile crust, so-called BD coupling (Brun, 1999). For given brittle crust thickness and ductile crust viscosity, the BD coupling increases with strain rate. Low BD-coupling (i.e., low strain rate) favors localized deformation (e.g., core complex mode) and, conversely, high BD-coupling (i.e., high strain rate) favors distributed deformation (e.g., wide rift mode). Laboratory experiments have demonstrated that a strain rate increase by a factor in the rank 3–5 is able to shift the extension from localized to distributed (Figure 4 in Brun, 1999). Therefore, we interpret the increase by a factor 5 of the mean strain rate in Southern Rhodope as responsible for the core complex segmentation by steep normal faults and associated basins (i.e., wide rift mode).

5.4. Pliocene-Quaternary Evolution of Basins and Reliefs

The northeastwardly increase of crustal thickness from 30–35 km in the southern part of the SRCC to around 40–45 km below the NRCC in Bulgaria (Boykova, 1999) indicates that crustal thickness has not yet been fully reequilibrated by SW directed extension. However, the present-day strong topographic gradients, as observed in the Pangeon with a maximum altitude of 2,000 m at 15 km from the seashore (Figure 4a) in an extending region, suggests reliefs supported by ductile crust flow (e.g., Block & Royden, 1991; Kruse et al., 1991). The MF that is responsible for Pangeon tilting and relief (Figure 13) was active in late Pliocene, indicating that the crust was still rather hot up to Pleistocene. However, since Pleistocene and likely due to

the propagation of the North Anatolian Fault in the North Aegean domain, the stretching direction changed from NE-SW to NS in whole North Greece (Lyberis, 1984; Mercier et al., 1987, 1989; see Figure 8 in Brun et al., 2016). Since this change in stretching direction, the magnitude of displacement rates strongly decreased in this region. Present-day strain rates calculated from Global Positioning System measurements (Pérouse et al., 2012) indicate that the Rhodope is still deforming but at very low strain rates. In addition, a 600-km-long profile, trending roughly NS, from the SE of Pannonian Basin and W of Dacic Basin, to the north, and Strymon Basin to the south indicates that the envelope of paleo-sea levels recorded by deltaic systems of Zanclean age (i.e., 3.5 Ma) has undergone a large wavelength undulation with altitudes ranging between 220 and 390 m (see Figures 13 and 14 in Suc et al., 2015). This indicates that, since Pliocene, the region is still deforming at very low strain rate, in agreement with Global Positioning System data, and has undergone a general uplift of 305 ± 85 m, in agreement with the positive dynamic topography induced by mantle flow that affects the North Aegean domain (see Figure 11 in Faccenna et al., 2014). In the Strymon Valley area, the two deltaic systems of Akropotamos and Serres display altitudes of 280 and 250 m above present-day sea level, respectively. The location of these deltaic systems along the northeastern side of the Strymon Basin indicates that, since Pliocene, deformation is controlled by the normal faults that bound the basin to the south (Figures 2 and 15).

5.5. Implications of Core Complex Segmentation in Geological Interpretation

The segmentation of a core complex by steep normal faulting and associated basin deposition as a result of an increase in stretching rate has, to our knowledge, never been neither described nor even invoked in the study of other core complexes. As there is no reason for such a process to be restricted to the Aegean back arc extension, we expect that a reexamination of brittle deformations superposed to structures and fabrics directly related to core complex exhumation in other field examples worldwide could lead to conclusions comparable to those expressed here. Besides the mechanical aspects discussed in sections 5.2 to 5.4, some implications, important for the geological interpretation of areas where core complexes are present, are worth being mentioned.

5.5.1. Basins

Since the earlier studies of core complexes (e.g., Crittenden Jr et al., 1978) it has been commonly admitted that sedimentary basins were deposited on detachment hanging wall. This is effectively often observed but not systematically. However, the fact that basins can also be deposited during segmentation of a core complex can be extremely misleading for the interpretation of core complexes, especially concerning the timing of their development. In the Rhodope, this has conducted many authors to assume that the contours of Neogene basins would represent a detachment, so-called "Strymon detachment." Interestingly, whereas it has been later recognized that the Kerdylion detachment better fit with the spectrum of cooling ages observed within the SRCC, from middle Eocene to lower Miocene, the Strymon Detachment has not been abandoned, even if it does not exist any strong and convincing evidence for its existence. Consequently, several recent papers consider that the two detachments have been successively involved in the exhumation of the SRCC (see Appendix A for details). In other words, it must not be assumed that sedimentary basins geographically associated to core complexes are not necessarily related to their detachment-controlled exhumation.

5.5.2. Segmentation of Core Complexes and Detachments

Normal faulting related to core complex segmentation can be responsible for strong reliefs, as demonstrated in the SRCC (Figure 4), and, close to sea level, pieces of a core complex can become islands, like Thassos (Figure 2) interpreted as *separate core complexes* (e.g., "Thassos Metamorphic Core Complex"; Wawrzenitz & Krohe, 1998). In central Aegean, the Cyclades archipelago resulted from the segmentation during Neogene of high pressure and high temperature metamorphic units previously exhumed (Brun et al., 2016). The Central Cyclades Core Complex is segmented in four main islands, each of them having been interpreted as a separate core complex, with its own detachment fault. Consequently, several distinct detachments are considered to occur whereas restoration of the geometry prior to Neogene segmentation suggests a single detachment at the scale of the whole Cyclades (Philippon et al., 2012).

5.5.3. Shear Criteria

Inside thick normal fault zones that controlled basin deposition semibrittle deformation lead to shear structures that can be used as shear criteria. In the MF (Figure 14) these structures indicate a sense of shear that trends almost perpendicular to the stretching lineation in gneiss mylonites, leaving no doubt on their relation

to postmetamorphic normal faulting. In fault zones trending perpendicular to the stretching lineation, like in faults located along the northern borders of the Drama Basin (Figure 8), such semibrittle shear structures trend almost parallel to the stretching lineation of gneiss mylonites and marbles. In this case, both generations of shear criteria that trend almost parallel cannot be easily separated if the fault zone is not identified on the basis of other observations. Therefore, some precautions must be taken in using shear criteria in domains where metamorphic rocks that became part of the brittle crust during exhumation have undergone faulting in a semibrittle rheological state. This should apply not only to segmented core complexes but more generally to all metamorphic rocks that underwent a tectonically controlled exhumation (e.g., within the blueschists and associated metamorphic sediments of the Cyclades, in the central Aegean Sea).

5.5.4. Geochronology and Cooling History

Blocking temperatures of isotopic systems are commonly used to construct time-temperature paths (i.e., cooling patterns) followed by metamorphic rocks during their exhumation in various types of tectonic settings. This has been largely used to describe the exhumation history of core complexes. However, in a core complex like the SRCC that has undergone a two-stage evolution, first of truly core complex-type exhumation followed by steep normal faulting (i.e., wide rifting), strong disturbances of low-temperature ages happen. This is illustrated in the SRCC by fission track data that kept the memory of earlier exhumation stages (Eocene-Oligocene) in the north and south of the core complex and much younger ages (Miocene) in the center of the core complex where steep normal faults controlled Neogene basin deposition (Figures 5 and 6). This has been used to argue in favor of the Strymon detachment (Kounov et al., 2015) even if it does not exist any field evidence for this detachment (see Appendix A for details). Consequently, a robust geological and structural analysis is a prerequisite for the interpretation of geochronological ages and for the construction of temperature-time paths. In other words, taking alone a set of geochronological ages, as good as it can be from an analytical point of view, cannot demonstrate the existence of any particular structure (e.g., a detachment/see section 3 in Appendix A). In addition, it could be extremely misleading to use ages from both high and low temperature geochronological methods in a single temperature-time path where two tectonic events followed one another, as different as core complex extension and wide rifting can be.

Appendix A: Time to Abandon the so-called "Strymon Detachment"

The concept of "Strymon Valley Detachment", also often called "Strymon Detachment," was introduced by Dinter and Royden (1993) in the following terms: "Along the northeast margin of the Strymon River valley in northeastern Greece, the primary contact between poorly consolidated Neogene sedimentary strata and underlying metamorphic and igneous rocks is a regionally developed low-angle normal fault, the Strymon Valley detachment, which can be traced along strike for more than 150 km from the Aegean coast near Kavala northwestward into the Struma Valley of Bulgaria." In other words, the contours of the Strymon Detachment according to this original definition correspond almost entirely to the contact between Neogene basins and metamorphic rocks, except to the south of the Drama basin where it is considered to be cut by a north-dipping normal fault. At variance with the above definition, Sokoutis et al. (1993; see their Figures 1 and 2) suggested that the core complex detachment was located in the Orfanos basin and extended within the Strymon Basin.

However, Brun and Sokoutis (2007) through structural mapping and using available petrological and geochronological data pointed out (i) that the contacts of Neogene basins with exhumed core units never correspond to a low-angle detachment but are either depositional or controlled by steep normal faults or by ramp-flat extensional systems (e.g., as exemplified in Thassos), (ii) that the core complex exhumation was controlled by the NS-trending Kerdylion detachment that separate the metamorphic core from the Serbo-Macedonian massif in the Chalkidiki peninsula (Figure 2), and (iii) that exhumation in the Kerdylion detachment footwall started in middle Eocene and not in late Oligocene-early Miocene. In addition, Brun and Sokoutis (2007) argued that field evidence used in favor of the Strymon Detachment in South Pangeon (Dinter & Royden, 1993) and in South Thassos (Wawrzenitz & Krohe, 1998; Figure 20a) in fact corresponds to a thrust, as earlier proposed by Kockel and Walther (1965), moderately reactivated in extension during the Neogene. In summary, the SRCC developed from middle Eocene controlled by the Kerdylion detachment and the extensional Neogene basins were superposed to the core complex since middle Miocene. Nevertheless, since 2007, the so-called Strymon detachment continued to be quoted in all

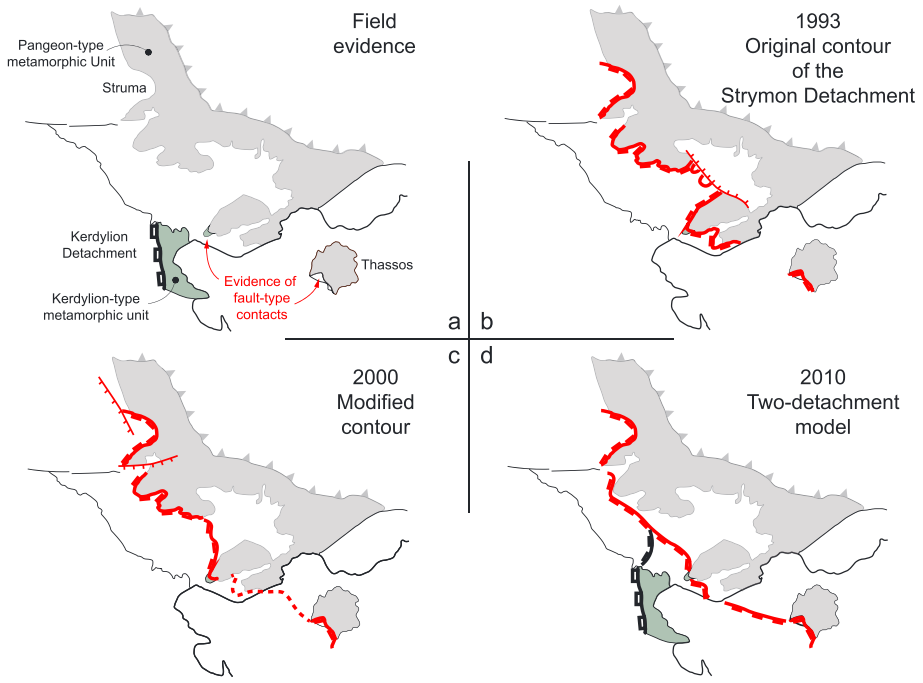

Figure 20. (a) The Strymon detachment concept. Location in southwest Pangeon and southwest Thassos of field evidence that were advocated in favor of the Strymon detachment. (b–d) Successive types of map contours of the Strymon detachment. See text for detailed explanation and complete references.

geological and tectonic regional studies by different working groups. Besides the present study of the relations between the core complex and the Neogene basins, in terms of processes, this appendix aims at clarifying why it would be appropriate to abandon the concept of Strymon Detachment.

A1. Various Map Contours for the Strymon Detachment

Since 1993, three main types of map contours have been used for the Strymon detachment. Krohe and Mposkos (2002), Burchfiel et al. (2008), Bonev et al. (2012), Punturo et al. (2014), and Stübner et al. (2016) use the Strymon Detachment contour initially proposed by Dinter and Royden (1993; Figure 20b). Conversely, some changes were introduced in other studies. Following Wawrzenitz and Krohe (1998), it was assumed that the detachment joins the southwest termination of the Pangeon to the southern end of the Menikion massif, partly hidden by recent sediments (Figure 20c; Burg, 2011; Kounov et al., 2010; Lips et al., 2000; Schenker et al., 2012; Tueckmantel et al., 2008; van Hinsbergen & Schmid, 2012). Fission tracks dating confirmed the existence of the Kerdylion Detachment and its activity since at least 42 Myr (Wüthrich, 2009). However, following Wüthrich (2009), a number of authors considered that both the Strymon detachment and the Kerdylion detachment have been involved in the exhumation of the SRCC (Froitzheim et al., 2014; Georgiev et al., 2010; Jahn-Awe et al., 2010, 2012; Janák et al., 2011; Kirchenbaur et al., 2012; Kounov et al., 2015; Nagel et al., 2011; Pleuger et al., 2011; Schmid et al., 2014; Figure 20d). According to this two-detachment model, the contour of the Strymon detachment, except to the southwest of the Pangeon and of Thassos, is entirely hidden below Neogene sediments, meaning that the contour of the sediments is not a low-angle detachment fault like in previous versions (Figures 20b and 20c). In summary, since its introduction in 1993, the Strymon detachment geometry has fluctuated in successive studies, indicating that the available field evidence (Figure 20a) were neither numerous nor robust enough to stabilize a common interpretation.

A2. The Contact Between the Kerdylion-Type Unit and the Pangeon-Type Unit Is Primarily a Thrust

Field evidence that have been invoked in favor of the Strymon detachment occur in only two domains of limited extent: in South Pangeon (Dinter & Royden, 1993) and in Southwest Thassos (Wawrzenitz & Krohe, 1998; Figure 20a). At both places, it is a southwest dipping contact between an upper unit made of gneisses and

migmatites and a lower unit made of marbles that is interpreted as a detachment. It must be recalled that this contact between the Kerdylion and the Pangeon units was initially interpreted as a thrust by Kockel and Walther (1965; see also geological map by Kockel et al., 1977). The oldest gneisses of the Kerdylion unit that rest on top of the Permian-Cretaceous marble pile of the Pangeon are Permo-Carboniferous (309–280 Ma; Himmerkus et al., 2006). This older-on-younger superposition confirms that the southwest-dipping Kerdylion-Pangeon contact is a thrust as proposed by Kockel and Walther (1965). In both Southwest Pangeon and Southwest Thassos, the thrust contact has been reactivated in extension, at least during the deposition of Neogene sediments, but reactivation remained moderate as it did not fully invert the older-on-younger superposition (Brun & Sokoutis, 2007). Therefore, this contact that is primarily a thrust cannot be considered as an extensional detachment.

At all other places, the contact between Neogene sediments and metamorphic rocks is either depositional or corresponds to steep normal faults (Figure 4b). Not a single outcrop has been found to bring evidence of a low-angle detachment at the base of Neogene basins. This should best explain why in 25 years the Strymon Detachment has not reached a common contour for all authors who attempted to draw it on a map (Figure 20).

A3. Relation Between Field Structural Evidence and Thermochronology Data

On the basis of low-temperature dating, Kounov et al. (2015) summarizes the double detachment interpretation (Figure 20d) in three steps: "The Kerdylion detachment initiated the exhumation of the SRCC at the latest at 42 Ma and controlled it until about 24 Ma. Between 24 and 12 Ma, the Strymon Valley detachment accommodated the exhumation. Since 12 Ma brittle normal faults, some of them cutting the Strymon Valley detachment were responsible for the final cooling of the basement rocks in the studied area and the formation of syn-tectonic sedimentary basins." Besides the fact that the Kerdylion-Pangeon contact is primarily a thrust and not a detachment, the ages of 24 and 12 Ma proposed for the onset and end of the detachment activity are weakly supported by data. The onset at 24 Ma relies on only one apatite FT age from a sample located close to Xanthi (i.e., close to the Nestos thrust), in the northern part of the core complex and about which the authors write: "The Strymon Valley detachment started to control the exhumation of the SRCC most probably after 24 Ma." Concerning the end at 12 Ma, they write: "Along the footwall, cooling from about 300 to below 60°C between ~17 and ~12 Ma is suggested from the combination of the zircon FT ages of samples close to the Strymon Valley detachment (RD63 Menikion, RD93 MF and RD88 North Thassos) and apatite FT ages of samples far from the detachment (sample GR2 Vrondou and those from the eastern slope of Pangeon Mt. and the inselbergs along the Drama basin)." This requires recalling some of field evidence described in this paper.

All zircon and apatite FT ages, attributed by Kounov and coworkers to the end of exhumation controlled by the Strymon Detachment, are located in the footwall of steep normal faults or in ramp-flat extensional systems that control sediment deposition in Neogene basins (see sections 4.1 [for "inselbergs along the Drama basin"], 4.2 [for RD 93 and "eastern slope of Pangeon"], and 4.3 [for RD 88]). RD 63 is not discussed in a specific section, but the sample is also located in the footwall of the major Anastasia normal fault that separates the Menikion massif from the Angitis basin (Figure 4).

Steep normal faulting and Neogene basin deposition occurred in a "hot" crust with a BD transition at a maximum depth of 7 km as indicated by (i) evidence of semibrittle behavior of gneisses and mylonites around the Drama basin (see section 4.1) and in the MF footwall (see section 4.2 and Figure 14) and (ii) the ductile behavior of marbles at shallow depths, in the range 2–3 km, allowing the development of ramp-flat extension in Alistrati (Figure 9c) and Thassos (Figure 18b). In the MF footwall, structure, kinematics, and FT ages indicate that the gneisses showing semibrittle behavior were at a temperature of around 300°C at a depth of 5 km at 12 Ma (Figure 13). In Thassos, the extensional décollement that accommodated the deposition of the Limenaria basin occurred around 13–12 Ma at a temperature of 300°C. The timing of extension in these two examples is in agreement with the Serravalian age of the oldest sediments in the Neogene basins. To the south of Drama Basin (in the above so-called "inselberg along the Drama basin"), apatite FT ages are older (from 16.5 to 18.5 Ma) than those obtained at other sites. However, considering the error bars that are rather large (from 4.4 to 4.8 Ma), they are not significantly different than Serravalian. The restoration of the Pangeon and Symvolon block tilting (Figure 13d) (i) shows that this faulting event starting in Serravalian or slightly before has been able to exhume rocks that were seated at 5 km depth and (ii) suggests that erosion

associated with block tilting reached up to 4.5 km in the Symvolon massif whose emplacement is dated at 20 Ma, bringing the SC-mylonites of the Symvolon granite to surface. Finally, Rb-Sr dating of Biotite indicates that the last ductile deformation in Thassos gneisses is in the range 14–15 Ma (Langhian) (Wawrzenitz & Krohe, 1998)—that is, immediately prior to oldest sediments in basins (Serravalian).

A4. Conclusion

In summary, it exists in favor of a Strymon detachment neither reliable field evidence nor obvious argument to choose 24 and 12 Ma as its possible onset and end of activity. Conversely, stratigraphic data in Neogene basins, detailed mapping of their internal structure and of normal faults that controlled their development, are in good agreement with all available FT ages and other geochronological data. From a more general point of view, it seems to us important to stress that deformation and related structures cannot be argued on the only basis of thermochronological and isotopic geochronological ages. Ages without a detailed assessment of their lithological and structural setting most often take the risk of being meaningless.

As documented in this paper, a two-stage evolution of the SRCC, first core complex-type controlled by the Kerdylion Detachment and second wide rift-type leading to the Neogene basins that segmented the core complex, explains all observations and measurements. This suggests that it is likely time to abandon the concept of Strymon Detachment.

Acknowledgments
Since we started to work in the Rhodope in the early 1990s we benefited from discussions with C. Burchfiel, J.-P. Burg, G. Clauson, C. Faccenna, D. Gapais, P. Gautier, F. Gueydan, L. Husson, L. Jolivet, D. Kostopoulos, L. Royden, L.E. Ricou, J.-P. Suc, and J. Van Den Driessche. Whereas some of them do not necessarily agree with some aspects of our interpretations, we are grateful to all of them for exchanges that helped us strengthen our analysis. We are also grateful to our students in PhD (K. Kydonakis and C. Tirel) and in MSc (C. Briend, M. Corver, and G. Estournes) who participated in the field and/or in the laboratory to some aspects of this work. We warmly thank the two reviewers J. Dewey and K. Soukis for their very positive comments and useful suggestions of improvement. Structural data used for this work are presented in maps and diagrams (Figures 4b, 8, 11a and 13a and 13b). Analytical results for Zircon and apatite fission tracks (Figures 5 and 6) can be found in Kounov et al. (2015, Table 1).

References

Bache, F., Popescu, S.-M., Rabineau, M., Gorini, C., Suc, J.-P., Clauzon, G., et al. (2011). A two-step process for the reflooding of the Mediterranean after the Messinian salinity crisis. *Basin Research*, *24*(2), 125–153. https://doi.org/10.1111/j.1365-2117.2011.00521.x

Berthé, D., Choukroune, P., & Jégouzo, P. (1979). Orthogneiss, mylonite and non coaxial deformation of granites: The example of the South Armorican shear zone. *Journal of Structural Geology*, *1*(1), 31–42. https://doi.org/10.1016/0191-8141(79)90019-1

Bestmann, M., Kunze, K., & Matthews, A. (2000). Evolution of a calcite marble shear zone complex on Thassos Island, Greece: Microstructural and textural fabrics and their kinematic significance. *Journal of Structural Geology*, *22*, 1789–1807.

Bigazzi, S. G., Christofides, G., Moro, A. D., & Kyriakopoulos, C. (1994). A contribution to the evolution of the Xanthi pluton (northern Greece): The apatite fission track analysis. *Bollettino della Societa Geologica Italiana*, *113*, 243–248.

Block, L., & Royden, L. (1991). Core complex geometries and regional scale flow in the lower crust. *Tectonics*, *9*, 557–567.

Bonev, N. (2006). Cenozoic tectonic evolution of the eastern Rhodope massif (Bulgaria): Basement structure and kinematics of syn- to post-collisional extensional deformation. *Special Paper of the Geological Society of America*, *409*, 211–235. https://doi.org/10.1130/2006.2409(12)

Bonev, N., Dilek, Y., Hanchar, J. M., Bogdanov, K., & Klain, L. (2012). Nd-Sr-Pb isotopic composition and mantle sources of Triassic rift units in the Serbo-Macedonian and the western Rhodope massifs (Bulgaria-Greece). *Geological Magazine*, *152*, 146–152.

Bornovas, J., & Rondogianni-Tsiambaou, T. (1983). *Geological map of Greece* (2nd ed., Sheets 2, scale 1:500 000). Athens: Institute of Geology and Mineral Exploration.

Bosse, V., Boulvais, P., Gautier, P., Tiepolo, P. M., Ruffet, G., Devidal, J. L., et al. (2009). Fluid-induced disturbance of the monazite Th-Pb chronometer: In situ dating and element mapping in pegmatites from the Rhodope (Greece, Bulgaria). *Chemical Geology*, *261*(3-4), 286–302. https://doi.org/10.1016/j.chemgeo.2008.10.025.

Boulvais, P., Brun, J.-P., & Sokoutis, D. (2007). Fluid circulation related to post-Messinian extension, Thassos island, North Aegean. *Geofluids*, *7*, 159–170.

Boykova, A. (1999). Moho discontinuity in central Balkan Peninsula in the light of the geostatistical structural analysis. *Physics of the Earth and Planetary Interiors*, *114*(1-2), 49–58. https://doi.org/10.1016/S0031-9201(99)00045-X

Brun, J.-P. (1999). Narrow rifts versus wide rifts: Inferences for the mechanics of rifting from laboratory experiments. *Philosophical Transactions of the Royal Society of London A*, *357*, 695–710.

Brun, J.-P., & Choukroune, P. (1983). Normal faulting, block tilting and décollement in a stretched crust. *Tectonics*, *2*(4), 345–356. https://doi.org/10.1029/TC002i004p00345

Brun, J.-P., & Faccenna, C. (2008). Exhumation of high-pressure rocks driven by slab rollback. *Earth and Planetary Science Letters*, *272*(1-2), 1–7. https://doi.org/10.1016/j.epsl.2008.02.038

Brun, J.-P., Faccenna, C., Gueydan, F., Sokoutis, D., Philippon, M., Kydonakis, K., & Gorini, C. (2016). The two-stage Aegean extension, from localized to distributed, a result of slab rollback acceleration. *Canadian Journal of Earth Sciences*, *53*(11), 1142–1157. https://doi.org/10.1139/cjes-2015-0203

Brun, J.-P., & Sokoutis, D. (2004). North Aegean extension: From the Rhodope core complex to Neogene basins. Paper presented at 5th International Symposium of Eastern Mediterranean Geology (pp. 49–52), Thessaloniki, Greece.

Brun, J.-P., & Sokoutis, D. (2007). Kinematics of the Southern Rhodope Core Complex (North Greece). *International Journal of Earth Sciences*, *96*(6), 1079–1099. https://doi.org/10.1007/s00531-007-0174-2

Brun, J.-P., & Sokoutis, D. (2010). 45 m.y. of Aegean crust and mantle flow driven by trench retreat. *Geology*, *38*(9), 815–818. https://doi.org/10.1130/G30950.1

Brun, J.-P., Sokoutis, D., Tirel, C., Gueydan, F., Van Den Driessche, J., & Beslier, M.-O. (2017). Crustal versus mantle core complexes. *Tectonophysics*. https://doi.org/10.1016/j.tecto.2017.09.017

Brun, J.-P., Sokoutis, D., & van den Driessche, J. (1994). Analogue modeling of detachment fault systems and core complexes. *Geology*, *22*(4), 319–322. https://doi.org/10.1130/0091-7613(1994)022%3C0319:AMODFS%3E2.3.CO;2

Buck, W. R. (1988). Flexural rotation of normal faults. *Tectonics*, *7*, 959–973. https://doi:10.1029/TC007i005p00959

Buck, W. R. (1991). Modes of continental lithospheric extension. *Journal of Geophysical Research*, *96*, 20,161–20,178. https://doi.org/10.1029/91JB01485

Burchfiel, B. C., Nakov, R., Dumurdzanov, N., Papanikolaou, D., Tzankov, T., Serafimovski, T., et al. (2008). Evolution and dynamics of the Cenozoic tectonics of the South Balkan extensional system. *Geosphere*, *4*(6), 919–938. https://doi.org/10.1130/GES00169.1

Burchfiel, B. C., Nakov, R., & Tzankov, T. (2003). Evidence from the Mesta half-graben, SW Bulgaria, for the Late Eocene beginning of Aegean extension in the Central Balkan Peninsula. *Tectonophysics*, *375*, 61–76.

Burg, J.-P. (2011). Rhodope: From Mesozoic convergence to Cenozoic extension, review of petro-structural data in the geochronological frame. In E. Skourtsos & G. S. Lister (Eds.), *The geology of Greece*, *Journal of the Virtual Explorer* (Vol. 39, pp. 1). https://doi.org/10.3809/jvirtex.5962011.00270

Burg, J.-P., Ricou, L.-E., Ivanov, Z., Godfriaux, I., Dimov, D., & Klain, L. (1996). Syn metamorphic nappe complex in the Rhodope massif. Structure and kinematics. *Terra Nova*, *8*(1), 6–15. https://doi.org/10.1111/j.1365-3121.1996.tb00720.x

Crittenden, M. D. Jr., Coney, P. J., & Davis, G. (1978). Tectonic significance of metamorphic cores complexes in the North American Cordillera. *Geology*, *6*(2), 79–80. https://doi.org/10.1130/0091-7613(1978)6%3C79:TSOMCC%3E2.0.CO;2

Dimitriadis, E. (1989). Sillimanite grade metamorphism in the Thassos Island, Rhodope Massif, Greece, and its regional significance. *Geolologica Rhodopica*, *1*, 190–201.

Dimitriadis, S., Kondopoulou, D., & Atzemoglou, A. (1998). Dextral rotation and tectonomagmatic evolution of the southern Rhodope and adjacent regions (Greece). *Tectonophysics*, *299*(1-3), 159–173. https://doi.org/10.1016/S0040-1951(98)00203-0

Dinter, D. A. (1998). Late Cenozoic extension of the Alpine collisional orogen, northeastern Greece: Origin of the north Aegean basin. *Geological Society of America Bulletin*, *110*(9), 1208–1230. https://doi.org/10.1130/0016-7606(1998)110%3C1208:LCEOTA%3E2.3.CO;2

Dinter, D. A., Macfarlane, A. M., Hames, W., Isachsen, C., Bowring, S., & Royden, L. (1995). U-Pb and 40Ar/39Ar geochronology of the Symvolon granodiorite: Implications for the thermal and structural evolution of the Rhodope metamorphic core complex, northeastern Greece. *Tectonics*, *14*(4), 886–908. https://doi.org/10.1029/95TC00926

Dinter, D. A., & Royden, L. (1993). Late Cenozoic extension in northeastern Greece: Strymon Valley detachment system and Rhodope metamorphic core complex. *Geology*, *21*(1), 45–48. https://doi.org/10.1130/0091-7613(1993)021%3C0045:LCEING%3E2.3.CO;2

Faccenna, C., Becker, T. W., Auer, L., Billi, A., Boschi, L., Brun, J.-P., et al. (2014). Mantle dynamics in the Mediterranean. *Reviews of Geophysics*, *52*, 283–332. https://doi.org/10.1002/2013RG000444

Faccenna, C., Jolivet, L., Piromallo, C., & Morelli, A. (2003). Subduction and the depth of convection in the Mediterranean mantle. *Journal of Geophysical Research*, *108*(B2), 2099. https://doi.org/10.1029/2001JB001690

Ferrière, J., Reynaud, J.-Y., Pavlopoulos, A., Bonneau, M., Migiros, G., Chanier, F., et al. (2004). Geologic evolution and geodynamic controls of the Tertiary intramontane piggyback Meso-Hellenic basin, Greece. *Bulletin de la Société Géologique de France*, *175*(4), 361–381. https://doi.org/10.2113/175.4.361

Froitzheim, N., Jahn-Awe, S., Frei, D., Wainwright, A. N., Maas, R., Georgiev, N., et al. (2014). Age and composition of meta-ophiolite from the Rhodope Middle Allochthon (Satovcha, Bulgaria): A test for the maximum-allochthony hypothesis of the Hellenides. *Tectonics*, *33*, 1477–1500. https://doi.org/10.1002/2014TC003526

Fytikas, M., Innocenti, F., Manetti, P., Mazzuoli, R., Peccerillo, A., & Villari, L. (1984). Tertiary to Quaternary evolution of volcanism in the Aegean region. In E. J. Dixon & A. H. F. Robertson (Eds.), *The geological evolution of the Eastern Mediterranean*, *Special Publication* (Vol. 17, pp. 687–699). London: Geological Society.

Galbraith, R. F., & Laslett, G. M. (1993). Statistical-models for mixed fission track ages. *Nuclear Tracks and Radiation Measurements*, *21*(4), 459–470. https://doi.org/10.1016/1359-0189(93)90185-C

Gapais, D. (1989). Shear structures within deformed granites: Thermal and mechanical indicators. *Geology*, *17*(12), 1144–1147. https://doi.org/10.1130/0091-7613(1989)017%3C1144:SSWDGM%3E2.3.CO;2

Gautier, P., Bosse, V., Cherneva, Z., Didier, A., Gerdjikov, I., & Tiepolo, M. (2017). Polycyclic alpine orogeny in the Rhodope metamorphic complex: The record in migmatites from the Nestos shear zone (N. Greece). *BSGF-Earth Sciences Bulletin*, *188*, 36. https://doi.org/10.1051/bsgf/2017195

Gautier, P., Gerdjikov, I., Ruffet, G., Bosse, V., Cherneva, Z., Pitra, P., & Hallot, E. (2009). Persistent synmetamorphic thrusting in the Rhodope until ca. 33 Ma: Evidence from the Nestos Shear Zone and implications for Aegean geodynamics, Abstracts Book (Vol. 1, p. 177), 62nd Geological Congress of Turkey, Ankara, April 2009.

Georgiev, N., Pleuger, J., Froitzheim, N., Sarov, S., Jahn-Awe, S., & Nagel, T. J. (2010). Separate Eocene-early Oligocene and Miocene stages of extension and core complex formation in the western Rhodopes, Mesta Basin, and Pirin Mountains (Bulgaria). *Tectonophysics*, *487*(1–4), 59–84. https://doi.org/10.1016/j.tecto.2010.03.009

Görür, N., & Okay, A. I. (1996). A fore-arc origin for the Thrace Basin, NW Turkey. *Geologische Rundschau*, *85*(4), 662–668. https://doi.org/10.1007/BF02440103

Gunnell, Y., Calvet, M., Meyer, B., Pinna-Jamme, R., Bour, I., Gautheron, C., et al. (2017). Cenozoic landforms and post-orogenic landscape evolution of the Balkanide orogen: Evidence for alternatives to the tectonic denudation narrative in southern Bulgaria. *Geomorphology*, *276*, 203–221. https://doi.org/10.1016/j.geomorph.2016.10.015

Gurk, M., Tougiannidis, N., Oikonomopoulos, I. K., & Kalisperi, D. (2015). The basement structure below the peat-lignite deposit in the Philippi sub-basin (northern Greece) inferred by electromagnetic and magnetic methods. *Journal of Applied Geophysics*, *115*, 40–50. https://doi.org/10.1016/j.jappgeo.2015.02.004

Hejl, E., Weingartner, H., Vavliakis, E., & Psilovikos, A. (1998). Macrorelief features and fission-track thermochronology of the Rila-Rhodope massif (eastern Macedonia, Greece). *Zeitschrift für Geomorphologie*, *42*, 517–530.

Himmerkus, F., Reischmann, T., & Kostopoulos, D. (2006). Late Proterozoic and Silurian basement units within the Serbo-Macedonian Massif, northern Greece: The significance of terrane accretion in the Hellenides. In A. H. F. Robertson & D. Mountrakis (Eds.), *Tectonic development of the Eastern Mediterranean Region*, *Special Publication* (Vol. 260, pp. 35–50). London: Geological Society. https://doi.org/10.1144/GSL.SP.2006.260.01.03

Jahn-Awe, S., Froitzheim, N., Nagel, T. J., Frei, D., Georgiev, N., & Pleuger, J. (2010). Structural and geochronological evidence for Paleogene thrusting in the western Rhodopes, SW Bulgaria: Elements for a new tectonic model of the Rhodope Metamorphic Province. *Tectonics*, *29*, TC3008. https://doi.org/10.1029/2009TC002558

Jahn-Awe, S., Pleuger, J., Frei, D., Georgiev, N., Froitzheim, N., & Nagel, T. J. (2012). Time constraints for low-angle shear zones in the central Rhodopes (Bulgaria) and their significance for the exhumation of high-pressure rocks. *International Journal of Earth Sciences*, *101*(7), 1971–2004. https://doi.org/10.1007/s00531-012-0764-5

Janák, M., Froitzheim, N., Georgiev, N., Nagel, T. J., & Sarov, S. (2011). P-T evolution of kyanite eclogite from the Pirin Mountains (SW Bulgaria): Implications for the Rhodope UHP metamorphic complex. *Journal of Metamorphic Geology*, *29*(3), 317–332. https://doi.org/10.1111/j.1525-1314.2010.00920.x

Jolivet, L., & Brun, J.-P. (2010). Cenozoic geodynamic evolution of the Aegean. *International Journal of Earth Sciences*, *99*(1), 109–138. https://doi.org/10.1007/s00531-008-0366-4

Jolivet, L., & Faccenna, C. (2000). Mediterranean extension and the Africa-Eurasia collision. *Tectonics*, *19*(6), 1095–1106. https://doi.org/10.1029/2000TC900018

Jones, C. E., Tarney, J., Baker, J. H., & Gerouki, F. (1992). Tertiary granitoids of Rhodope, Northern Greece: Magmatism related to extensional collapse of the Hellenic orogen. *Tectonophysics*, *210*, 295–314. https://doi.org/10.1016/0040-1951(92)90327%E2%80%933

Karakitsios, V., Cornée, J. J., Tsourou, T., Moissette, P., Kontakiotis, G., Agiadi, K., et al. (2017). Messinian salinity crisis record under strong freshwater input in marginal, intermediate, and deep environments: The case of the North Aegean. *Palaeogeography, Palaeoclimatology, Palaeoecology*, *485*, 316–335. https://doi.org/10.1016/j.palaeo.2017.06.023

Kaufman, P. S. (1995). Extensional tectonic history of the Rhodope metamorphic core complex, Greece and geophysical modeling of the Halloran Hills, California, (PhD thesis). (295 pp.). Cambridge: Massachusetts Institute of Technology.

Kilias, A., & Mountrakis, D. (1990). Kinematics of the crystalline sequences in the western Rhodope massif. In S. Konstantinos (Ed.), *Proceedings, 2nd Hellenic-Bulgarian Symposium, Thessaloniki, 1989*, *Geologica Rhodopica* (Vol. 2, pp. 100–116). Thessaloniki: Aristotle University Press.

Kirchenbaur, M., Pleuger, J., Jahn-Awe, S., Nagel, T. J., Froitzheim, N., Fonseca, R. O. C., & Münker, C. (2012). Timing of high-pressure metamorphic events in the Bulgarian Rhodopes from Lu-Hf garnet geochronology. *Contributions to Mineralogy and Petrology*, *163*(5), 897–921. https://doi.org/10.1007/s00410-011-0705-5

Kissel, C., & Laj, C. (1988). The Tertiary geodynamic evolution of the Aegean Arc: A palaeomagnetic reconstruction. *Tectonophysics*, *146*(1-4), 183–201. https://doi.org/10.1016/0040-1951(88)90090-X

Kockel, F., Mollat, H., & Walther, H. W. (1977). *Erläuterungen zur Geologischen Karte der Chalkidhiki und angrenzender Gebiete 1:100 000 (Nord-Griechenland)* (p. 119). Hannover: Bundesanstalt für Geowissenschaften und Rohstoffe.

Kockel, F., & Walther, H. W. (1965). Die Strimonlinie als Grenze zwischen Serbo-Mazedonischem und Ril-Rhodope-Massiv in Ost-Mazedonien. *Geologisches Jahrbuch*, *83*, 575–602.

Kolocotroni, C., & Dixon, J. E. (1991). The origin and emplacement of the Vrondou granite, Serres, N.E. Greece. *Bulletin of the Geological Society of Greece*, *25*, 469–483.

Koukouvelas, I., & Doutsos, T. (1990). Tectonic stages along a traverse cross cutting the Rhodopian zone (Greece). *Geologische Rundschau*, *79*(3), 753–776. https://doi.org/10.1007/BF01879213

Kounov, A., Seward, D., Burg, J.-P., Bernoulli, D., Ivanov, Z., & Handler, R. (2010). Geochronological and structural constraints on the Cretaceous thermotectonic evolution of the Kraishte zone (western Bulgaria). *Tectonics*, *29*, TC2002. https://doi.org/10.1029/2009TC002509

Kounov, A., Wüthrich, E., Seward, D., Burg, J.-P., & Stockli, D. (2015). Low-temperature constraints on the Cenozoic thermal evolution of the southern Rhodope Core Complex (northern Greece). *International Journal of Earth Sciences (Geol Rundsch)*, *104*(5), 1337–1352. https://doi.org/10.1007/s00531-015-1158-2

Kousparis, D. (1979). Seismic stratigraphy and basin development—Nestos Delta area, northeastern Greece. (PhD thesis), University of Tulsa: USA.

Krohe, A., & Mposkos, E. (2002). Multiple generations of extensional detachments in the Rhodope mountains (Northern Greece) evidence of episodic exhumation of high-pressure rocks. *Geological Society of London, Special Publication*, *204*, 151–178. https://doi.org/10.1144/GSL.SP.2002.204.01.10

Kruse, S., McNutt, M., Phipps-Morgan, J., Royden, L., & Wernicke, B. (1991). Lithospheric extension near Lake Mead, Nevada: A model for ductile flow in the lower crust. *Journal of Geophysical Research*, *96*, 4435–4456.

Kydonakis, K., Brun, J.-P., & Sokoutis, D. (2015). North Aegean core complexes, the gravity spreading of a thrust wedge. *Journal of Geophysical Research, Solid Earth*, *120*, 595–616. https://doi.org/10.1002/2014JB011601

Kydonakis, K., Brun, J.-P., Sokoutis, D., & Gueydan, F. (2015). Kinematics of Cretaceous subduction and exhumation in the western Rhodope (Chalkidiki block). *Tectonophysics*, *665*, 218–235. https://doi.org/10.1016/j.tecto.2015.09.034

Kydonakis, K., Gallagher, K., Brun, J.-P., Jolivet, M., Gueydan, F., & Kostopoulos, D. (2014). Upper Cretaceous exhumation of the western Rhodope Metamorphic Province (Chalkidiki Peninsula, northern Greece). *Tectonics*, *33*, 1113–1132. https://doi.org/10.1002/2014TC003572

Kyriakopoulos, K. G., Magganas, A. C., Norelli, P., Bigazzi, G., Del Moro, A., & Kokkinakis, A. (1996). Thermochronological evolution of symvolon and pangeon plutons and their country rocks, Kavala area, N. Greece; an apatite fission track analysis. *Neues Jahrbuch fuer Mineralogie*, *11*, 519–529.

Lalechos, N. (1986). Correlations and observations in molassic sediments in onshore and offshore areas of northern Greece. *Lithos*, *56*, 89–99.

Liati, A. (2005). Identification of repeated Alpine (ultra) high pressure metamorphic events by U-Pb SHRIMP geochronology and REE geochemistry of zircon: The Rhodope zone of northern Greece. *Contributions to Mineralogy and Petrology*, *150*(6), 608–630. https://doi.org/10.1007/s00410-005-0038-3

Liati, A., & Gebauer, D. (1999). Constraining the prograde and retrograde P-T-t path of Eocene rocks by SHRIMP dating of different zircon domains: Inferred rates of heating, burial, cooling and exhumation for central Rhodope, northern Greece. *Contributions to Mineralogy and Petrology*, *135*(4), 340–354. https://doi.org/10.1007/s004100050516

Lips, A. L. W., White, S. H., & Wijbrans, J. R. (2000). Middle-late Alpine thermotectonic evolution of the southern Rhodope Massif, Greece. *Geodinamica Acta*, *13*(5), 281–292. https://doi.org/10.1080/09853111.2000.11105375

Lyberis, N. (1984). Tectonic evolution of the north Aegean trough. In J. E. Dixon & A. H. F. Robertson (Eds.), *The geological evolution of the Eastern Mediterranean*, *Special Publication* (Vol. 17, pp. 709–725). London: Geological Society. https://doi.org/10.1144/GSL.SP.1984.017.01.57

Lyberis, N., & Sauvage, J. (1985). Evolution tectonique de la region nord égéenne (Grece) du Pliocene au Pleistocene. *Bulletin de la Société Géologique de France*, *8*, 581–595.

Mascle, J., & Martin, L. (1990). Shallow structure and recent evolution of the Aegean Sea: A synthesis based on continuous reflection profiles. *Marine Geology*, *94*(4), 271–299. https://doi.org/10.1016/0025-3227(90)90060-W

McClusky, S., Balassanian, S., Barka, A., Demir, C., Ergintav, S., Georgiev, I., et al. (2000). Global Positioning System constraints on plate kinematics and dynamics in the eastern Mediterranean and Caucasus. *Journal of Geophysical Research*, *105*, 5695–5719. https://doi.org/10.1029/1999JB900351

Mercier, J.-L., Sorel, D., & Simeakis, K. (1987). Change in the state of stress in the overriding plate of a subduction zone: The Aegean Arc from the Pliocene to the present. *Annales Tectonicae*, *1*, 20–39.

Mercier, J.-L., Sorel, D., Vergely, P., & Simeakis, K. (1989). Extensional tectonic regimes in the Aegean basins during the Cenozoic. *Basin Research*, *2*(1), 49–71. https://doi.org/10.1111/j.1365-2117.1989.tb00026.x

Nagel, T. J., Schmid, S., Janak, M., Froitzheim, N., Jahn-Awe, S., & Georgiev, N. (2011). The exposed base of a collapsing wedge: The Nestos Shear Zone (Rhodope Metamorphic Province, Greece). *Tectonics*, *30*, TC4009. https://doi.org/10.1029/2010TC002815

Nalpas, T., & Brun, J.-P. (1993). Salt flow and diapirism related to extension at crustal scale. *Tectonophysics*, *228*, 349–362. https://doi.org/10.1016/0040-1951(93)90348-N

Papanikolaou, D. (2013). Tectonostratigraphic models of the Alpine terranes and subduction history of the Hellenides. *Tectonophysics*, *595-596*, 1–24. https://doi.org/10.1016/j.tecto.2012.08.008

Pe-Piper, G., & Piper, D. J. W. (2006). Unique features of the Cenozoic igneous rocks of Greece. *Geological Society of America, Special Paper*, *409*, 259–281.

Pérouse, E., Chamot-Rooke, N., Rabaute, A., Briole, P., Jouanne, F., Georgiev, I., & Dimitrov, D. (2012). Bridging onshore and offshore present-day kinematics of central and eastern Mediterranean: Implications for crustal dynamics and mantle flow. *Geochemistry, Geophysics, Geosystems*, *13*, Q09013. https://doi.org/10.1029/2012GC004289

Philippon, M., Brun, J. P., & Gueydan, F. (2012). Deciphering subduction from exhumation in the segmented Cycladic Blueschist Unit (central Aegean, Greece). *Tectonophysics*, *524-525*, 116–134. https://doi.org/10.1016/j.tecto.2011.12.025

Pleuger, J., Georgiev, N., Jahn-Awe, S., Froitzheim, N., & Valkanov, N. (2011). Kinematics of Palaeogene low-angle extensional faults and basin formation along the eastern border of the central Rhodopes (Bulgaria). *Zeitschrift der Deutschen Gesellschaft für Geowissenschaften*, *162*(2), 171–192. https://doi.org/10.1127/1860-1804/2011/0162-0171

Proedrou, P., & Papaconstantinou, C. M. (2004). *Prinos basin—A model for oil exploration*, *Bulletin of the Geological Society of Greece* (Vol. 36, pp. 327–333). Thessaloniki: Proceedings of the 10th International Congress.

Punturo, R., Cirrincione, R., Fazio, E., Fiannacca, P., Hartmut, K., Mengel, K., et al. (2014). Microstructural, compositional and petrophysical properties of mylonitic granodiorites from an extensional shear zone (Rhodope Core complex, Greece). *Geological Magazine*, *151*(6), 1051–1071. https://doi.org/10.1017/S001675681300109X

Ricou, L.-E., Burg, J.-P., Godfriaux, I., & Ivanov, Z. (1998). Rhodope and Vardar: The metamorphic and the olistostromic paired belts related to the Cretaceous subduction under Europe. *Geodinamica Acta*, *11*(6), 285–309. https://doi.org/10.1080/09853111.1998.11105326

Roussos, N. (1994). Stratigraphy and paleogeographic evolution of Palaeocene molassic basins of N. Aegean. *Bulletin of the Geological Society of Greece*, *30*(2), 275–294.

Royden, L. H. (1993). The tectonic expression slab pull at continental convergent boundaries. *Tectonics*, *12*(3), 629–638. https://doi.org/10.1029/92TC02641

Schenker, F. L., Gerya, T., & Burg, J.-P. (2012). Bimodal behavior of extended continental lithosphere: Modeling insight and application to thermal history of migmatitic core complexes. *Tectonophysics*, *579*, 88–103. https://doi.org/10.1016/j.tecto.2012.07.002

Schmid, S. M., Bernoulli, D., Fügenschuh, B., Geogiev, N., Kounov, A., Matenco, L., et al. (2014). Tectonic units of the Alpine collision zone between Eastern Alps and Western Turkey, Geological Map.

Snel, E., Mărunțeanu, M., & Meulenkamp, J. E. (2006). Calcareous nannofossil biostratigraphy and magnetostratigraphy of the upper Miocene and lower Pliocene of the northern Aegean (Orphanic Gulf-Strimon Basin areas), Greece. *Palaeogeography, Palaeoclimatology, Palaeoecology*, *238*(1-4), 125–150. https://doi.org/10.1016/j.palaeo.2006.03.022

Sokoutis, D., Brun, J.-P., van Den Driessche, J., & Pavlides, S. (1993). A major Oligo-Miocene detachment in southern Rhodope controlling north Aegean extension. *Journal of the Geological Society, London*, *150*(2), 243–246. https://doi.org/10.1144/gsjgs.150.2.0243

Stübner, K., Drost, K., Schoenberg, R., Böhme, M., Starke, J., & Ehlers, T. A. (2016). Asynchronous timing of extension and basin formation in the south Rhodope core complex, SW Bulgaria, and northern Greece. *Tectonics*, *35*(1), 136–159. https://doi.org/10.1002/2015TC004044

Suc, J.-P., Popescu, S.-M., Do Couto, D., Clauzon, G., Rubino, J.-L., Melinte-Dobrinescu, M. C., et al. (2015). Marine gateway vs. fluvial stream within the Balkans from 6 to 5 Ma. *Marine and Petroleum Geology*, *66*, 231–245. https://doi.org/10.1016/j.marpetgeo.2015.01.003

Tirel, C., Brun, J.-P., & Burov, E. (2008). Dynamics and structural development of metamorphic core complexes. *Journal of Geophysical Research*, *113*, B04403. https://doi.org/10.1029/2005JB003694

Tirel, C., Brun, J.-P., Burov, E., Wortel, M. J. R., & Lebedev, S. (2013). A plate tectonics oddity: Caterpillar-walk exhumation of subducted continental crust. *Geology*, *41*, 555–558. https://doi.org/10.1130/G33862.1

Tirel, C., Brun, J.-P., & Sokoutis, D. (2006). Extension of thickened and hot lithospheres: Inferences from laboratory modeling. *Tectonics*, *25*, TC1005. https://doi.org/10.1029/2005TC001804

Tranos, M. D. (2011). Strymon and Strymonikos Gulf basins (northern Greece): Implications on their formation and evolution from faulting. *Journal of Geodynamics*, *51*(4), 285–305. https://doi.org/10.1016/j.jog.2010.10.002

Tranos, M. D. (2016). Slip preference analysis of faulting driven by strike-slip Andersonian stress regimes: An alternative explanation of the Rhodope metamorphic core complex (northern Greece). *Journal of the Geological Society*, *174*(1), 129–141. https://doi.org/10.1144/jgs2015-164

Tranos, M. D., Eleftheriadis, G. E., & Kilias, A. A. (2009). Philippi granitoid as a proxy for the Oligocene and Miocene crustal deformation in the Rhodope Massif (eastern Macedonia, Greece). *Geotectonic Research*, *96*(1), 69–85. https://doi.org/10.1127/1864-5658/09/96-0069

Tueckmantel, C., Schmidt, S., Neisen, M., Georgiev, N., Nagel, T. J., & Froitzheim, N. (2008). The Rila-Pastra normal fault and multi-stage extensional unroofing in the Rila Mountains (SW Bulgaria). *Swiss Journal of Geosciences*, *101*(Supplement 1), 295–310. https://doi.org/10.1007/s00015-008-1287-8

Turpaud, P., & Reischmann, T. (2010). Characterisation of igneous terranes by zircon dating: Implications for UHP occurrences and suture identification in the central Rhodope, northern Greece. *International Journal of Earth Sciences*, *99*(3), 567–591. https://doi.org/10.1007/s00531-008-0409-x

van Hinsbergen, D. J. J., & Schmid, S. M. (2012). Map view restoration of Aegean-west Anatolian accretion and extension since the Eocene. *Tectonics*, *31*, TC5005. https://doi.org/10.1029/2012TC003132

von Quadt, A., & Peytcheva, I. (2005). The southern extension of the Srednogorie type Upper Cretaceous magmatism in Rila-western Rhodopes: Constraints from isotope geochronological and geochemical data. In *Proc. Intern. Conf. 80th Anniversary of the Bulgarian Geological Society, Sofia* (pp. 113–116).

Wawrzenitz, N., & Krohe, A. (1998). Exhumation and doming of the Thasos metamorphic core complex (S. Rhodope, Greece): Structural and geochronological constraints. *Tectonophysics*, *285*, 301–332. https://doi.org/10.1016/S0040-1951(97)00276-X

Weingartner, H., & Heijl, E. (1994). The relief generations of Thasos and the first attempt of fission track dating in Greece, 7th Congr. Geological Society of Greece (1994), p. 105 Abstract.

Wernicke, B., & Axen, G. (1988). On the role of isostasy in the evolution of normal fault systems. *Geology*, *16*(9), 848–851. https://doi.org/10.1130/0091-7613(1988)016%3C0848:OTROII%3E2.3.CO;2

Wüthrich, E. D. (2009). Low temperature thermochronology of the northern Aegean Rhodope Massif, (PhD thesis). (p. 99), ETH Zürich.